**Dynamics of Carbon and Water Fluxes in the Southern United States in Responses to Changes in Climate and Atmospheric Composition during 1900-2099**

by

Xia Song

A thesis submitted to the Graduate Faculty of
Auburn University
in partial fulfillment of the
requirements for the Degree of
Master of Science

Auburn, Alabama
August 6, 2011

Key words: Atmospheric Composition, Carbon, Climate Change,
Southern United States, Water



Approved by

Hanqin Tian, Chair, Alumni Professor of Forestry and Wildlife Sciences
Greg Somers, Associate Professor of Forestry and Wildlife Sciences
Luke J. Marzen, Associate Professor of Geography

Abstract

The southern United States (SUS) has experienced dramatic changes in climate, atmospheric composition, and land cover type over the past century. These changes are expected to be continuous in this century, which may substantially alter the structure and function of terrestrial ecosystems and then affect the regional carbon and water fluxes in the SUS. Thus, understanding the dynamics of carbon and water in the terrestrial ecosystems across the SUS in response to historical and projected changes in climate and atmospheric composition is essential for wisely dealing with future climate change and maintaining the sustainability of human society. Based on our previous study which investigated the changes in carbon and water fluxes in the SUS over the 20$^{th}$ century in the context of multifactor global change, this research further investigated the potential changes in carbon and water fluxes under the projected changes in climate and atmospheric composition during 2010-2099, by using a process-based ecosystem model-Dynamic Land Ecosystem Model (DLEM). The simulation results indicate that net primary productivity (NPP) over the SUS increased from 1900 to 2099, while net ecosystem productivity (NEP) increased from 1900 to 2080s and then decreases; ET increased before the 1970s, and then decreased to the 2020s, and increases to the 2080s before a decline. There are inter-annual variations of simulated NPP, NEP, and ET over the study period. The NPP-based WUE kept relatively stable before the 1950s and then increases by the end of the 21$^{st}$ century; and the NEP-based WUE increased from the 1900s to the 2080s with large inter-annual variations, and then decline after the 2080s.

Under the projected climate change, the NPP decreases under A2 scenario, keeps relatively stable under B1 scenario, while increases under A1B scenario over the time period of 2010-2099; the NEP decreases under all three scenarios, with the highest decrease under A2 scenario, and the lowest decrease under B1 scenario; the ET increases under all three scenarios, with the highest increase under A1B scenario, and lowest increase under B1 scenario.

This study is among the first attempts to examine the spatiotemporal variations of carbon and water fluxes over the SUS in the context of multiple factor global change in the 21$^{st}$ century. The results obtained in this study might improve the understanding of both the public and scientific community on the effects of future global change. The factorial attribution of the variations of carbon and water fluxes over the SUS would provide insights for policy makers who aim to mitigate and adapts to global change. Since the changes in climate and atmospheric composition are inevitable in the near future, it is critical to assess and explore the management strategies to ensure the adaptation of terrestrial ecosystems in the SUS to these changes.

Acknowledgments

This study has been supported by DOE National Institute of Climate Change Research (DUKE UN-07-SC-NICCR-1016) and NASA IDS (NNG04GM39C).

First of all, I wish to express my gratitude to Dr. Hanqin Tian for his academic advice throughout the course of my three years of study and research at Auburn University. I would sincerely appreciate all support from my committee: Drs. Greg Somers and Luke J. Marzen for their invaluable comments on my thesis.

My special gratitude goes to Ms. Shufen Pan, who helped me a lot on both research work and daily life, Drs. Mingliang Liu, Chi Zhang, Wei Ren, Guangsheng Chen, Chaoqun Lu, Bo Tao, Wenquan Zhu, Huiqin Mao, Guiying Li, Wenhui Kuang, and Jun Li, for their inciting discussion and communication on scientific questions. I thank Mr. Qichun Yang and Mr. Jia Yang for communication on scientific and technical issues during my study.

I also want to express my thanks to Ms. Patti Staudenmaier, and all the faculty and staff in the School of Forestry and Wildlife Sciences.

I am deeply grateful to my family, my mom, who raises me and supports me all the time, my Husband, Dr. Xiaofeng Xu, my daughter, Grace Songya Xu, and my son, Henry Songyi Xu, for their continually love, support and understanding. They are the source of happiness in my life.

Last but certainly not least, I would also thank all the people I know or do not know who yielded direct and indirect impacts on me.

Table of Contents

List of Tables

List of Figures

List of Abbreviations

| | |
|---|---|
| AR | Autotrophic respiration |
| ET | Evapotranspiration |
| GFDL | Geophysical Fluid Dynamic Laboratory |
| GISS | Goddard Institute for Space Studies |
| GPP | Gross primary production |
| HR | Heterotrophic respiration |
| NCAR | National Center for Atmospheric Research |
| NEP | Net Ecosystem Production |
| NPP | Net Primary Production |
| SUS | Southern United States |
| UKMO | United Kingdom Meteorological Office |
| WUE | Water Use Efficiency |
| WUE_NPP | Water Use Efficiency expressed as the ratio of NPP and ET |
| WUE_NEP | Water Use Efficiency expressed as the ratio of NEP and ET |

# Chapter 1 Introduction

Over the past decades, global change has become one of the most important problems facing human society, and drawn attentions from both the public and the scientific community (Vitousek et al., 1997). Global change involves changes of a number of environmental factors including climate system, air pollution, land-use and land cover types, and elevated atmospheric $CO_2$, etc (Heimann and Reichstein, 2008; Vitousek et al., 1997). Primarily caused by human activities, these environmental factors have evolved dramatically and affected the Earth system over the past century (Heimann and Reichstein, 2008; Vitousek et al., 1997; Denman et al., 2007); yet their effects on the terrestrial ecosystems are still far from certain (Heimann and Reichstein, 2008; Tian et al., 2010a).

The anthropogenic activities, such as fossil fuel combustion and deforestation, have caused the increase of atmospheric $CO_2$ concentration from 280 ppm in preindustrial time (Neftel et al., 1982; Friedli et al., 1986) to 380 ppm at present; and the atmospheric $CO_2$ concentration is expected to reach 700 ppm or higher towards the end of the 21st century (Solomon et al., 2007). The elevated atmospheric $CO_2$ and other greenhouse gases resulted in a 0.76°C increase of the Earth's surface temperature over the past 150 years, and a further increase of 1.5-6.4 $^{o}$C by the end of the 21st century is expected (Solomon et al., 2007). Climate change also includes the alterations of precipitation regimes across time and space. Global precipitation is anticipated to increase by approximately 0.5-1% per decade in the 21$^{st}$ century (Solomon et al., 2007). These changes may cause a substantial change of ecosystem functions, in particular,

carbon sequestration (Cramer et al., 2001; Fang et al., 2005; Heimann and Reichstein 2008). A number of studies have concluded that the net carbon losses from the terrestrial biosphere might cause the amplification rather than the dampening of current climatic change (Cox et al., 2000; Friedlingstein et al., 2003, 2006).

The carbon and water cycles are tightly coupled through stomatal behavior (Chapin et al., 2002; Jackson et al., 2005), and both fluxes could generate feedbacks on atmosphere and climate system such as $CO_2$ concentration, precipitation patterns and sensible/latent heating etc. A number of field observations have been conducted to examine the effects of global change on carbon and water fluxes in terrestrial ecosystems (Thomas et al., 2010; Medvigy et al., 2010; Janssens et al., 2010; Immerzeel et al., 2010). The earliest long-term $CO_2$ measurements were conducted over different sites across the globe in the early 1990s (Black et al. 1996; Greco and Baldocchi 1996; Valentini et al. 1996; Wofsy et al. 1993; Yamamoto et al. 1999). Since they are site-level studies, it is inappropriate to directly extrapolate to the region. Thus, it is necessary to combine all the measurement sites in a network. Soon, regional networks were launched around the globe, such as AmeriFlux and Fluxnet-Canada in North America (Coursolle et al. 2006; Margolis et al. 2006), the Large Biosphere Amazon (LBA) in South America (Keller et al. 2004), the EuroFlux in Europe (Ciais et al. 2005; Valentini et al. 2000), OzFlux in Australia, China Flux in China (Yu et al. 2006), AsiaFlux in Asia and AfriFlux in Africa (www.fluxnet.ornl.gov). Scientists used the eddy flux data to examine the biological and environmental controls on water flux, carbon flux and water use efficiency (Yu et al., 2008; Baldocchi et al., 1996, 2001).

One major shortcoming of these field experiments is the limitation in temporal and spatial scales. A modeling approach could be used to overcome this limitation and estimate ecosystem functioning at large-scales over long time periods (Melillo et al., 1993; Tian et al.,

2008). Over the past decades, ecosystem models have been broadly used to study the carbon and water cycles in response to global environmental changes (Morales et al., 2005; Tian et al., 2010a; Schimel et al., 2000; Melillo et al., 1993). Prentice et al. (2001) classified process-based models into two types: terrestrial biogeochemical models (TBMs) and dynamic global vegetation models (DGVMs). The TBMs simulate the fluxes of carbon, water and nitrogen within terrestrial ecosystems; the DGVMs couple carbon, nitrogen and water processes with changes in slow ecosystem processes depending on resource competition, establishment, growth and mortality of different plant functional types. These models can be used to simulate the effects of projected climate change on terrestrial ecosystems, which may differ from the present in many aspects including changes in water availability, seasonality of precipitation, etc.

A large number of modeling studies have been conducted to assess regional water and carbon cycles under the effects of climate change (Nemani et al. 1993; Running 1994; Houghton et al. 1998; Randerson et al. 1997), soil carbon dynamics (Motovalli et al. 1994), atmospheric nitrogen input (Aber et al. 1997), ozone pollution (Ren et al., 2007), and land use/cover change (Liu et al., 2008). However, few studies simultaneously considered multiple global change factors such as elevated atmospheric $CO_2$, ozone pollution, nitrogen input, and climate change (Ren et al., 2007; Tian et al., 2010a, 2010b). In a previous study, Tian et al. (2010a) modeled these global change factors and concluded that the multifactor global change increased the net primary production, evaportranspiration, and WUE in the southern United States (SUS) over the time period of 1895-2007.

The SUS, has been considered as the largest carbon sink among the six major bioclimatic regions of the conterminous United States (Schimel et al. 2000). It has a large potential to continuously function as a substantial carbon sink in the future because of the large area of

young pine forests (Turner et al. 1995; Birdsey et al. 2006; Malmsheimer et al. 2008). However, the population in this area has been increasing due to the immigration of people from other areas and the local population growth. This increase in population will cause substantial changes in the structure of terrestrial ecosystems and thus affect the regional carbon dynamics which will further contribute to climate change. As reported, terrestrial ecosystems in the SUS have experienced multiple stresses including changes in land use/land cover (Wear 2002; Chen et al. 2006), climate changes, and land management practices (Houghton et al. 1999; Dale et al. 2001; Chen et al. 2006), and those factors have dramatically influenced carbon dynamics in agricultural land and forests from site-level to regional scales (Tian et al., 2010a). All these environmental changes will be continuously yielding effects on land ecosystems over the SUS in the 21$^{st}$ century. To understand the potential effects of and adapt to these changes in atmosphere and environment, it is critically important to examine the carbon and water fluxes in the SUS in the context of multiple-factor global change in the 21$^{st}$ century.

In this study the terrestrial ecosystem models (DLEM: Dynamic Land Ecosystem Model) was applied to examine the impacts of changes in climate and atmospheric compositions on carbon and water fluxes. The major objectives of this study were:

1) To examine the temporal and spatial patterns of carbon and water fluxes and WUE in terrestrial ecosystems under changes in climate system (temperature and precipitation) and atmospheric composition ($CO_2$, N deposition, and $O_3$) during 1900-2099 in the SUS.
2) To attribute the variations in carbon and water fluxes to individual global change factors and their interactive effects on the temporal scale from 2010 to 2099.

The above two questions were addressed by analyzing the results as simulated by DLEM over the time period of 1900-2099, with emphasis on 2010 - 2099. The global change factors

include climate variability, elevated atmospheric $CO_2$, $O_3$ pollution, and nitrogen deposition for the time period of 1900-2099, and the land use change for the time period of 1900-2009.

# Chapter 2 Study Region, Input Data and Methodology

## 2.1. Study Region

The SUS region spans from 75$^{o}$ W to 100$^{o}$ W in longitude and from 30$^{o}$ N to 37$^{o}$ N in latitude. The elevation of this region ranges from near sea level along the Gulf and Atlantic coasts to more than 1800 m in the Appalachian Mountains. Over the SUS, the summer seasons are relatively long, hot, and humid, with very small day-to-day fluctuation in temperature. Normally, local afternoon thundershowers occur very commonly from late June to mid-August. The cold season includes December, January, and February, although severely cold weather is rare (Cooter 1992).

The major forest types in this region are temperate coniferous forest and temperate deciduous forest; the contemporary vegetation map in the year of 2005 is shown in Figure 1. The northeastern part of the SUS (Virginia, Kentucky, Tennessee, and North Carolina) and Arkansas are dominated by temperate deciduous forest. Texas mainly features shrub and desert, and coniferous forest dominates forest land in the South Carolina, Georgia, and Alabama, Mississippi, and Louisiana (Fig. 1).

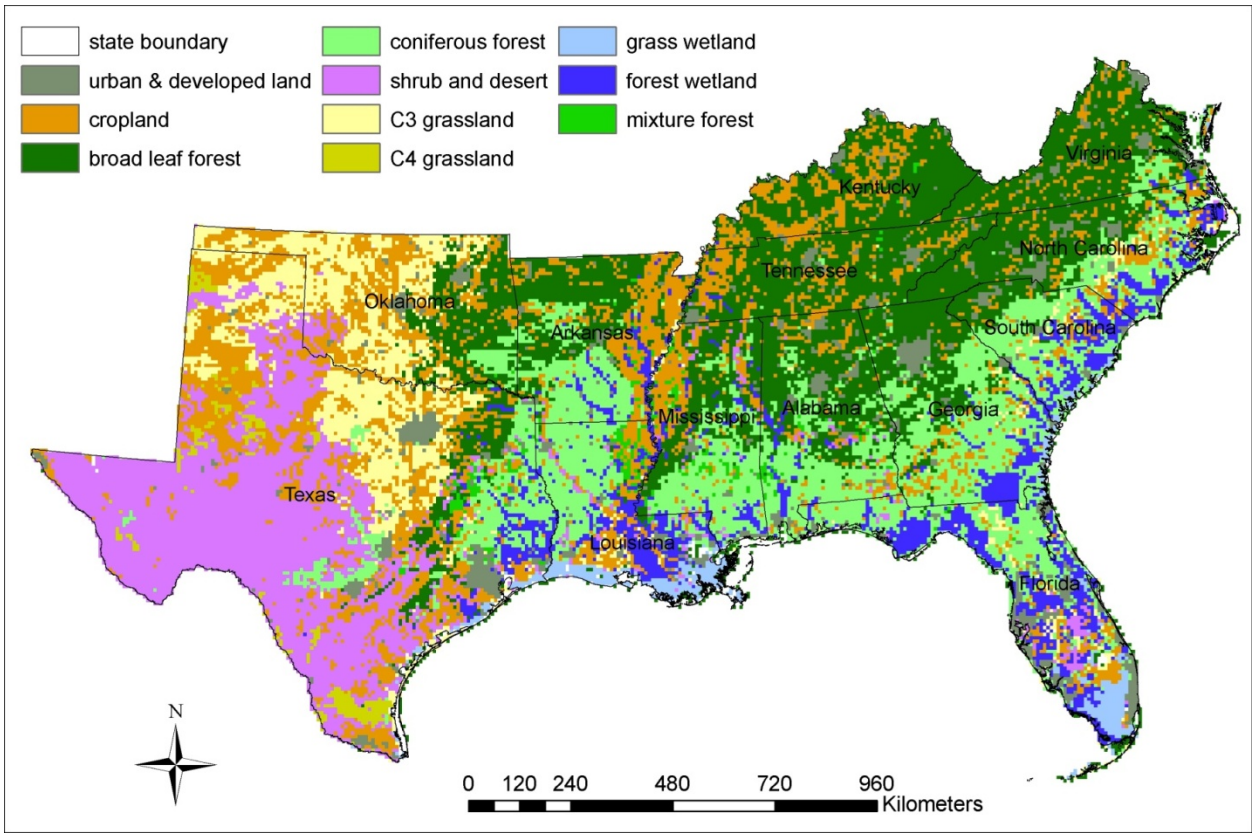


Figure 1 The boundary and contemporary vegetation of the Southern US (cited from Tian et al., 2010a; Zhang et al., 2008)

## 2.2. Model Description

Process-based ecosystem models, which consider the physiological responses to changes in atmospheric composition and climate, have proved to be powerful in examining ecosystem responses to multiple environmental stresses, especially at a regional scale (Tian et al., 1998, 2002, 2003, 2010a, 2010b, 2010c; Karnosky et al., 2005). In this study, a process-based ecosystem, Dynamic Land Ecosystem Model (DLEM), was used to assess the historical and future carbon and water fluxes in the SUS in response to changes in climate and atmospheric composition. DLEM is a highly-integrated process-based terrestrial ecosystem model that simulates carbon, nitrogen, and water cycles at a daily time step. It is driven by changes in atmospheric chemistry such as ozone pollution and nitrogen deposition, climate variability, $CO_2$

concentration, land-use and land-cover types and disturbances (i.e., fire, hurricane, and harvest) (Fig 2).

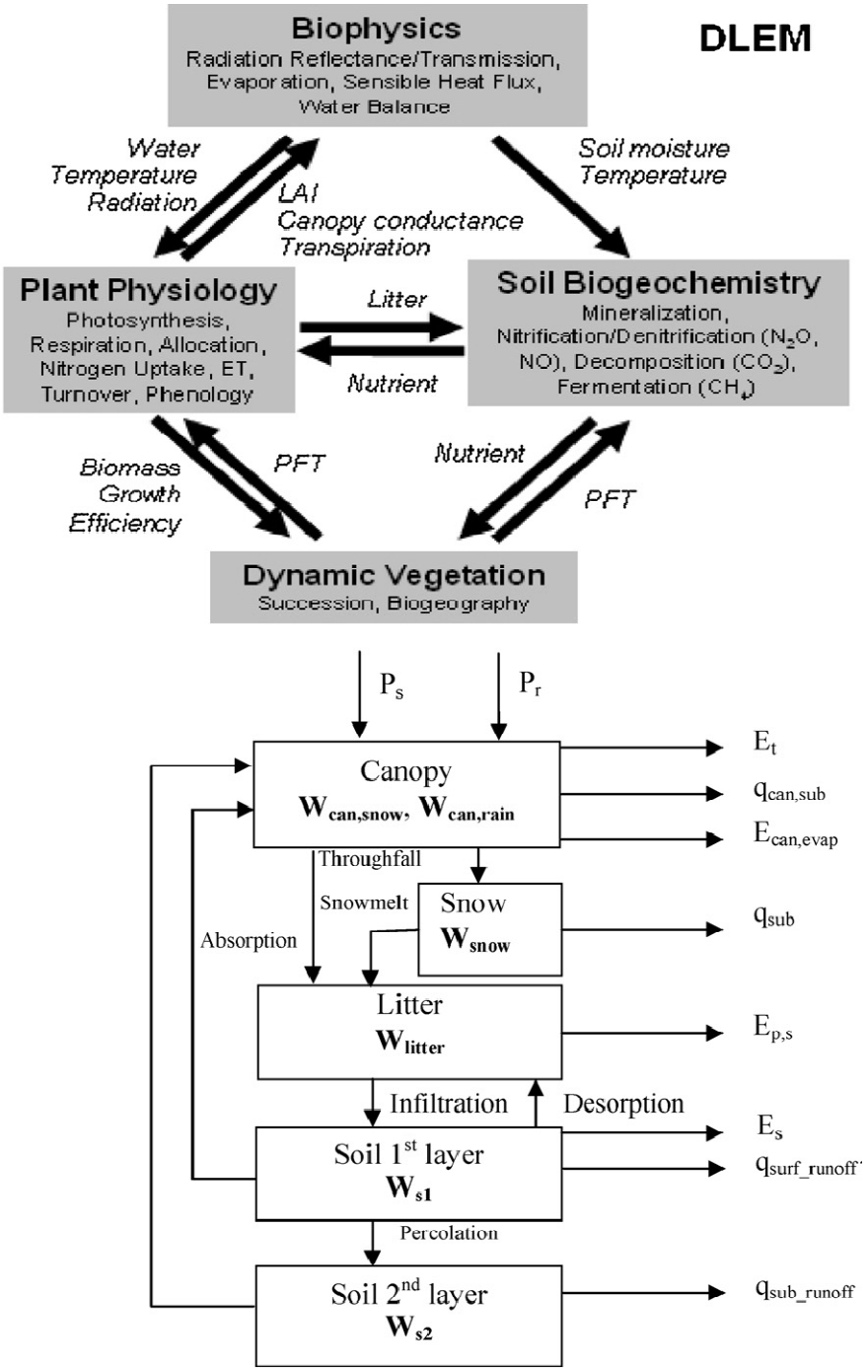


Figure 2 Framework (upper one) and the hydrological components (below one) of the Dynamic Land Ecosystem Model (From Tian et al., 2010a)

Note: The soil is represented by three layers: a litter layer (or above surface water) with varied depth, and two mineral soil layers with fixed depths of 0.5 m (0–50 cm) and 1.0 m (50–150 cm), respectively. Snow (Ps) and rain (Pr) are separated from precipitation. Canopy intercepts some of Ps and Pr into canopy snow storage (Wcan, snow) and rain storage (Wcan, rain), respectively. The intercepted water is eventually evaporated (Ecan, evap) or sublimated (qcan, sub) to the air. The remaining Ps and Pr enter into the ground snowpack (Wsnow) and litter layer (Wlitter) as throughfall. The Wlitter is over maximum water storage of the litter, extra water will be infiltrated into the first soil layer. Simultaneously, the litter layer will absorb water from the first soil layer. The water holding by the litter will be evaporated to air (Ep,s). When the soil moisture in first mineral layer (Ws1) exceeds the saturated soil water content, the extra water will run off from this layer which forms surface runoff (qsurf, runoff) or infiltrate in the second soil layer (Ws2). The water in the first soil layer will be evaporated into air (Es). The water percolation from the second soil layer forms subsurface runoff (qsurf, runoff).

DLEM emphasizes the modeling and simulation of managed ecosystems including agricultural ecosystems, plantation forests and pastures. The spatially-explicit management data sets, such as irrigation, fertilization, rotation, and harvest can be used as input information for controlling the ecosystems. It also simulates urbanization processes, and can be used to estimate the impacts of urban impervious surface and urban lawn management on ecosystem processes.

The basic simulation unit of DLEM is a single grid with corresponding coverage area. In this unit, vegetated land surfaces are comprised of one of the natural vegetation functional types (forests, grassland and shrubs) or urban area or cropping system. The classification of natural forests is based on the leaf structure (needle and broadleaf), leaf phenology (evergreen and deciduous), climate zones (tropical, temperate, and boreal). The grasslands are divided into C3 grass, C4 grass, and meadow. The shrubs have evergreen and deciduous types. Besides, other plant functional types including desert, wetland and tundra are also considered.

For simulating vegetation dynamics, DLEM model uses a strategy similar to the dynamic global vegetation model (DGVM) LPJ. The time step for vegetation dynamic processes is one year. Two kinds of vegetation dynamic processes can be simulated by DLEM: the biogeography redistribution due to climate change, and the plant competition and succession during vegetation

recovery after disturbances. Like most DGVMs, DLEM builds on the concept of plant functional types (PFT) to describe vegetation distributions. Many different PFTs that adapt to local climate can coexist in the same grid, competing for light, water, and nutrient resources. For the historical simulations, which focus on historical variations of carbon, nitrogen, and water cycles affected by changing climate, land-use, and atmospheric compositions, the prescribed plant functional type for natural vegetation cover or human-managed systems, like cropland and urban were used.

In the DLEM, water in terrestrial ecosystems is classified into six pools: the canopy intercepted snow and intercepted water; the ground surface snow; the litter intercepted water; the upper layer soil water (0 ~ 50 cm), and the lower layer soil water (50 ~ 150 mm). The water content in each boxes are updated daily based on water input (precipitation and dew) and the water losses (evaporation, transpiration, sublimation, surface runoff and drainage runoff) (unit mm/day) driven by the solar radiation and the plant's physiological processes. The major processes include the partition of precipitation, canopy interception of rain and snow, canopy snow sublimation, snowmelt and sublimation from ground snowpack, canopy evapotranspiration, litter interception of rain or snow, soil surface evaporation, surface runoff and infiltration, and soil moisture movement.

The carbon cycle is the most important process in the DLEM; it serves as a framework for biogeochemical processes of other nutrients and hydrological processes. The DLEM mainly simulates carbon fluxes through various pools. The vegetation carbon pool has six components for trees and shrubs (storage organ, leaf, heartwood, sapwood, fine root, and coarse root), and five components for herbaceous vegetation (storage organ, leaf, stem, fine root, and coarse root). Vegetation carbon pool gains carbon through photosynthesis (Gross Primary Production, GPP), looses carbon through autotrophic respiration (including maintenance respiration and growth

respiration), litter fall, mortality, and disturbances such as land conversion and fire. The effects of ozone pollution and nitrogen deposition on photosynthesis are also simulated in the DLEM. The litter carbon pool includes seven pools for trees and shrubs: coarse woody debris, aboveground very active litter, aboveground middle active litter, aboveground resistant litter, belowground very active litter, belowground middle active litter, and belowground resistant litter. The sources of litter pools include litterfalls from leaves and roots, debris from mortalities, harvest, and land use change. Litter carbon pools can be converted into soil organic matter (SOM) pools and emits $CO_2$ to the atmosphere through decomposition.

Soil organic matter has three pools with different decomposition base rate: very active, middle active, resistant SOM, and dissolved organic carbon. The balance of SOM depends on the transformation of litter to SOM, the fractions of conversion from GPP to the dissolved organic carbon (DOC), the returned organic matter from production decay (e.g. manure), the growth of microbes, the methane production from DOC, and the decomposition rate. Meanwhile, the DLEM simulates the life cycles of microbe. It should be noted that the methane module in the DLEM mainly simulates the production, consumption, and transport of $CH_4$ (Tian et al., 2010a).

DLEM has been used to investigate the responses of terrestrial carbon and water cycles to multiple stresses including changes in climate, atmospheric composition ($CO_2$, nitrogen deposition, and surface ozone), and land use/cover change patterns in Asia (Tian et al., 2003, 2008, Ren et al., 2007), North America (Tian et al., 2010b, Xu et al., 2010) and the SUS (Tian et al., 2010a).

In this study, the simulations span a 200-year timeframe from 1900 to 2099 at a spatial resolution of 8 km by 8 km. Twenty-seven simulations were designed to investigate the impacts of multiple stresses on the carbon and water fluxes in the SUS (Table 1).

Table 1 The simulation experiments to investigate the impacts of multiple global change factors on carbon and water fluxes across the Southern US from 1900 to 2099

| Scenarios Code | | | Climate Change | $CO_2$ Change | $O_3$ Change | Nitrogen deposition Change | Note |
|---|---|---|---|---|---|---|---|
| Climate | Model | Scenarios | | | | | |
| | GFDL | A1B | 1900-2099 | 1900-2010 | 1900-2010 | 1900-2010 | Single Factor |
| | GFDL | A2 | 1900-2099 | 1900-2010 | 1900-2010 | 1900-2010 | Single Factor |
| | GFDL | B1 | 1900-2099 | 1900-2010 | 1900-2010 | 1900-2010 | Single Factor |
| | NCAR | A1B | 1900-2099 | 1900-2010 | 1900-2010 | 1900-2010 | Single Factor |
| | NCAR | A2 | 1900-2099 | 1900-2010 | 1900-2010 | 1900-2010 | Single Factor |
| | NCAR | B1 | 1900-2099 | 1900-2010 | 1900-2010 | 1900-2010 | Single Factor |
| | GISS | A1B | 1900-2099 | 1900-2010 | 1900-2010 | 1900-2010 | Single Factor |
| | GISS | A2 | 1900-2099 | 1900-2010 | 1900-2010 | 1900-2010 | Single Factor |
| | GISS | B1 | 1900-2099 | 1900-2010 | 1900-2010 | 1900-2010 | Single Factor |
| | UKMO | A1B | 1900-2099 | 1900-2010 | 1900-2010 | 1900-2010 | Single Factor |
| | UKMO | A2 | 1900-2099 | 1900-2010 | 1900-2010 | 1900-2010 | Single Factor |
| | UKMO | B1 | 1900-2099 | 1900-2010 | 1900-2010 | 1900-2010 | Single Factor |
| $CO_2$ | | | 1900-2010 | 1900-2099 | 1900-2010 | 1900-2010 | Single Factor |
| $O_3$ | | | 1900-2010 | 1900-2010 | 1900-2099 | 1900-2010 | Single Factor |
| Nitrogen deposition | | | 1900-2010 | 1900-2010 | 1900-2010 | 1900-2099 | Single Factor |
| GFDLA1B_$CO_2$_$O_3$_NDEP | | | 1900-2099 | 1900-2099 | 1900-2099 | 1900-2099 | Overall |
| GFDLA2_$CO_2$_$O_3$_NDEP | | | 1900-2099 | 1900-2099 | 1900-2099 | 1900-2099 | Overall |
| GFDLB1_$CO_2$_$O_3$_NDEP | | | 1900-2099 | 1900-2099 | 1900-2099 | 1900-2099 | Overall |
| NCARA1B_$CO_2$_$O_3$_NDEP | | | 1900-2099 | 1900-2099 | 1900-2099 | 1900-2099 | Overall |

| | | | | | |
|---|---|---|---|---|---|
| NCARA2_$CO_2$_$O_3$_NDEP | 1900-2099 | 1900-2099 | 1900-2099 | 1900-2099 | Overall |
| NCARB1_$CO_2$_$O_3$_NDEP | 1900-2099 | 1900-2099 | 1900-2099 | 1900-2099 | Overall |
| GISSA1B_$CO_2$_$O_3$_NDEP | 1900-2099 | 1900-2099 | 1900-2099 | 1900-2099 | Overall |
| GISSA2_$CO_2$_$O_3$_NDEP | 1900-2099 | 1900-2099 | 1900-2099 | 1900-2099 | Overall |
| GISSB1_$CO_2$_$O_3$_NDEP | 1900-2099 | 1900-2099 | 1900-2099 | 1900-2099 | Overall |
| UKMOA1B_$CO_2$_$O_3$_NDEP | 1900-2099 | 1900-2099 | 1900-2099 | 1900-2099 | Overall |
| UKMOA2_$CO_2$_$O_3$_NDEP | 1900-2099 | 1900-2099 | 1900-2099 | 1900-2099 | Overall |
| UKMOB1_$CO_2$_$O_3$_NDEP | 1900-2099 | 1900-2099 | 1900-2099 | 1900-2099 | Overall |

Note: The time period of 1900-2099 indicates that the data for the time period of 1900-2099 was used in the simulations; while the time period of 1900-2010 indicates that the data for the period of 1900-2010 was used in the simulations and the post-2010 simulations were fed by the data of the year 2010; NDEP: nitrogen deposition.

### 2.3. Input Data

In this study, the model input data include daily climate data (1900-2099), annual historical land-use and land-cover maps (1900-2005), annual atmospheric $CO_2$, daily tropospheric ozone concentrations (1900-2099), annual nitrogen deposition (1900-2050), annual nitrogen fertilizer application in cropland (1900-2005), and soil property maps. All the geospatial data were reprojected to equal-areal Albert projection at a spatial resolution of 8 km × 8 km to drive the DLEM model (Table 2).

Table 2 The input data required by Dynamic Land Ecosystem Model in model simulations

| Category | Data | Unit | Type | Temporal Resolution | Time Span |
|---|---|---|---|---|---|
| Background data | Potential vegetation | DB[1], CB[2], AS[3], G[4] | Base map | | |
| | Soil clay content | % | Base map | | |

| | | | | | |
|---|---|---|---|---|---|
| | Soil sand content | % | Base map | | |
| | Soil silt content | % | Base map | | |
| | Soil depth | m | Base map | | |
| | Soil acidity | pH | Base map | | |
| | Soil bulk density | g /$cm^3$ | Base map | | |
| | Elevation map | m | Base map | | |
| | Aspect map | Degree | Base map | | |
| | Slope map | Degree | Base map | | |
| | Irrigation map | 0/1 | Base map | | |
| Historical data | Precipitation | mm / year | Climatic data | Daily | 1865-2009 |
| | Temperature_Avg | Celsius | Climatic data | Daily | 1865-2009 |
| | Temperatue_Max | Celsius | Climatic data | Daily | 1865-2009 |
| | Temperature_Min | Celsius | Climatic data | Daily | 1865-2009 |
| Future data | Precipitation | mm / year | Climatic data | Daily | 2010-2099 |
| | Temperature_Avg | Celsius | Climatic data | Daily | 2010-2099 |
| | Temperatue_Max | Celsius | Climatic data | Daily | 2010-2099 |
| | Temperature_Min | Celsius | Climatic data | Daily | 2010-2099 |
| Historical data | $CO_2$ | ppmv | Atmospheric data | Annual | 1865-2007 |
| | Ozone concentration AOT40[5] | ppb-hr | Atmospheric data | Daily | 1865-2005 |
| | Nitrogen deposition (NHx) | mgN $m^{-2}$ $y^{-1}$ | Atmospheric data | Annual | 1865-2005 |
| | Nitrogen deposition (NHy) | mgN $m^{-2}$ $y^{-1}$ | Atmospheric data | Annual | 1865-2005 |
| Future data | $CO_2$ | ppmv | Atmospheric data | Annual | 2008-2099 |
| | Ozone concentration AOT40[5] | ppb-hr | Atmospheric data | Daily | 2006-2099 |
| | Nitrogen deposition (NHx) | mgN $m^{-2}$ $y^{-1}$ | Atmospheric data | Annual | 2006-2050* |
| | Nitrogen deposition (NHy) | mgN $m^{-2}$ $y^{-1}$ | Atmospheric data | Annual | 2006-2050* |
| Historical data | Nitrogen Fertilization | gN $m^{-2}$ $y^{-1}$ | Land-use data | Annual | 1895-2005 |
| Historical data | Cropland distribution | 0/1 | Land-use data | Annual | 1895-2005 |

Note: 1: deciduous broadleaf; 2: coniferous broadleaf forest; 3: arid shrub land; 4: grassland; 5: AOT40 (ppb-hr) is the accumulated dose over a threshold of 40 ppb during daylight hours; * the post-2050 nitrogen deposition was kept constant as the year 2005.

*2.3.1 Climate Data*

One important advantage of DLEM is that it requires relatively few input datasets. For example, a minimum climate dataset like precipitation, maximum temperature, mean temperature, and minimum temperature will be enough to drive the model. In this study, the climate data span two hundred years (1900-2099). With 2010 as a cutoff year, the climate data were separated into two time periods: a historical climate dataset covering 1865-2009 and a future climate dataset covering 2010-2099. It should be noted that the historical climate data used in this study are different from Tian et al. (2010a); the climate variables used in this study include minimum temperature, maximum temperature, average temperature, and precipitation, while Tian et al. (2010a) used the climate variable dew point besides variables used in this study. This study uses temperature and precipitation to keep consistent with projected climate dataset simulated by GCMs.

**Historical Climate Dataset:**

In a previous study (Tian et al., 2010a), the climate data at a spatial resolution of 8 km × 8 km for the entire SUS region was developed by integrating the daily climate pattern of North American Regional Reanalysis (NARR) dataset (http://wwwt.emc.ncep.noaa.gov/mmb/rreanl/) that covers the period of 1979 to 2007, with the monthly long-term (1900 to 2007) historical climate dataset developed by PRISM (Parameter-elevation Regressions on Independent Slopes Model) Group at Oregon State University (OSU) (http://prism.oregonstate.edu/) (Zhang, 2008). The daily values prior to 1979 were estimated by defining the following variables for each month in the NARR dataset:

$$P_T = T_d - T_m \qquad \text{equation 1.1}$$

$$P_P = P_d / P_m \qquad \text{equation 1.2}$$

where $P_T$ and $P_P$ were daily pattern of the temperature and precipitation, respectively; $T_d$ and $P_d$ were the NARR daily temperature (mean, maximum, and minimum temperature) and precipitation, respectively; and $T_m$ and $P_m$ were the NARR monthly average temperature (mean, maximum, and minimum temperature) and monthly total precipitation, respectively. Then, for the period before 1979, each year used a randomly selected annual climate pattern dataset from those estimated from the NARR dataset. Finally, the selected climate pattern was used to expand the monthly climate data to PRISM to construct the daily climate dataset:

$$T_{d'} = P_T + T_{m'} \qquad \text{equation 1.3}$$

$$P_{d'} = P_p * P_{m'} \qquad \text{equation 1.4}$$

where $T_{d'}$ and the $P_{d'}$ were the derived daily temperature (mean, maximum, and minimum temperature) and precipitation, respectively; $P_T$ and $P_P$ are the daily pattern of the temperature and precipitation, and $T_{m'}$ and $P_{m'}$ are the PRISM monthly average temperature and monthly total precipitation, respectively. Since the PRISM data starts from 1895, the climate data covering 1895-2009 was generated. To extend the dataset back to 1865 for model spinning-up purpose, each year was randomly chosen from 1961-1990. In this study, the data was extended from 2007 to 2009 by using the same method adopted by Zhang (Zhang, 2008).

**Future Climate Data**:

For the future climate dataset, monthly temperature, precipitation data (2010-2099) based on 4 climate models (GFDL_CM2_1, GISS_MODEL_E_R, NCAR_CCSM3_0, UKMO_HADCM3) and three greenhouse gas emissions scenarios (A1B, A2, and B1) were downloaded from the website: http://gdo-dcp.ucllnl.org/downscaled_cmip3_projections/. The detailed downscale technique from monthly to daily in temporal and from $0.5^o$ to 8km in spatial is described by Maurer et al (2007). The climate data for simulation included the following variables:

- Precipitation; mm/day (daily).
- Average daily air temperature; deg C (daily).
- Maximum daily air temperature, deg C (daily).
- Minimum daily air temperature, deg C (daily).

Three different scenarios broadly used in the IPCC report were selected for this study (IPCC, 2001, 2007).

- A1B: “the A1 storyline and scenario family describes a future world of very rapid economic growth, global population that peaks in mid-century and declines thereafter, and the rapid introduction of new and more efficient technologies. Major underlying themes are convergence among regions, capacity building, and increased cultural and social interactions, with a substantial reduction in regional differences in per capita income. The A1 scenario family develops into three groups that describe alternative directions of technological change in the energy system. The three A1 groups are distinguished by their technological emphasis: fossil intensive (A1FI), non-fossil energy sources (A1T), or a balance across all sources (A1B).”
- A2: “the A2 storyline and scenario family describes a very heterogeneous world. The underlying theme is self-reliance and preservation of local identities. Fertility patterns across regions converge very slowly, which results in continuously increasing global population. Economic development is primarily regionally oriented and per capita economic growth and technological change is more fragmented and slower than in other storylines.”
- B1: “the B1 storyline and scenario family describes a convergent world with the same global population that peaks in midcentury and declines thereafter, as in the A1 storyline,

but with rapid changes in economic structures toward a service and information economy, with reductions in material intensity, and the introduction of clean and resource-efficient technologies. The emphasis is on global solutions to economic, social, and environmental sustainability, including improved equity, but without additional climate initiatives."

--------*P18 of the IPCC report* (IPCC, 2007: Summary for Policymakers. In: Climate Change 2007: The Physical Science Basis. Contribution of Working Group I to the Fourth Assessment Report of the Intergovernmental Panel on Climate Change [Solomon, S., D. Qin, M. Manning, Z. Chen, M. Marquis, K.B. Averyt, M.Tignor and H.L. Miller (eds.)]. Cambridge University Press, Cambridge, United Kingdom and New York, NY, USA).

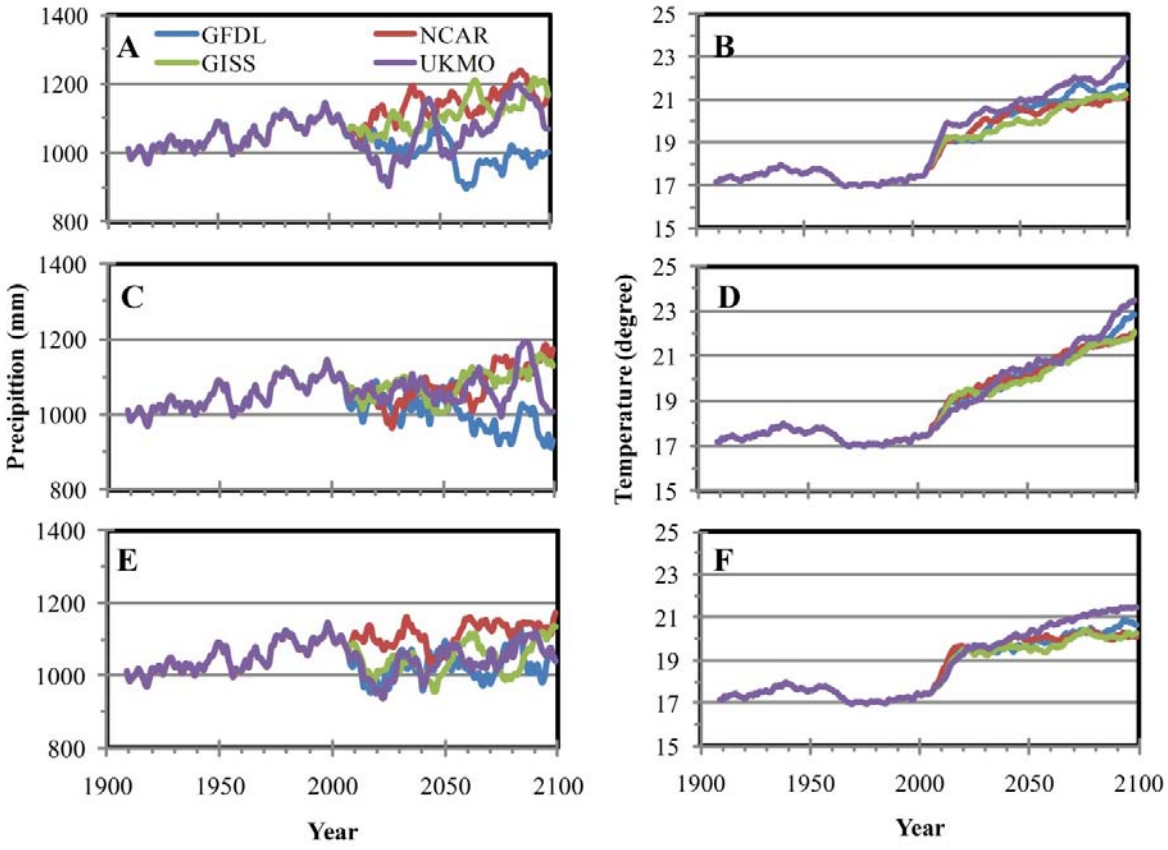


Figure 3 Temporal variations of annual average temperature and precipitation under three scenarios estimated by four climate models during 1900 to 2099 (A: precipitation under the A1B scenario; B: temperature under the A1B scenario; C: precipitation under the A2 scenario; D: temperature under the A2 scenario; E: precipitation under the B1 scenario; F: temperature under the B1 scenario)

The temporal patterns of precipitation and temperature over the past 110 years and future 90 years simulated by different models under three scenarios are illustrated in Figure 3 and are summarized in the Figure 4. During the historical time period of 1900-2009, the precipitation fluctuated until the 1940s, with an increase up to the 2000s; while the temperature increased before the 1940s, decreased to the 1980s, and then increased to the 2010s.

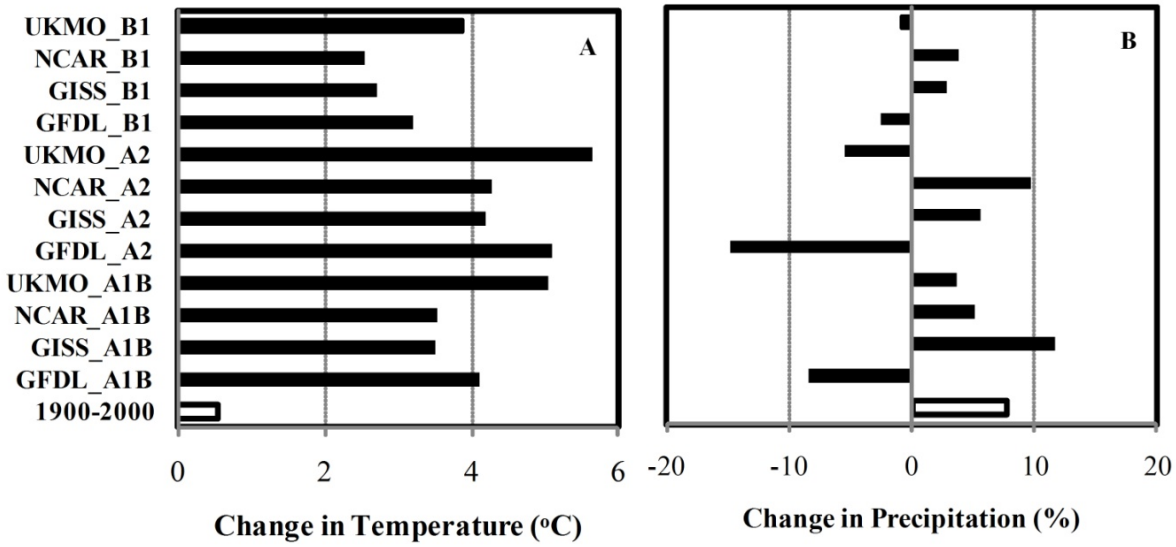


Figure 4 Changes of (A) temperature and (B) precipitation from the 2000s to the 2090s (for the comparison, the changes from 1900s to the 2000s are shown at the bottom of Figure 4A and 4B)

For the projected climate scenarios, there are large discrepancies among climate scenarios and models. Overall, the A2 climate scenario shows the highest temperature increase, A1B climate scenario shows medium temperature increase while B1 climate scenario shows the lowest temperature increase (Fig 4). For the projected temperature, the results simulated by UKMO model under A2 scenario show the largest change, increasing approximately 5.7 $^{o}$C from the 2000s to the 2090s; the results simulated by NCAR under B1 scenario show the smallest change, increasing approximately 2.6 $^{o}$C from the beginning to the end of the 21$^{st}$ century. According to these results, the changes in temperature over the future 90 years are larger than

those over the past 110 years. The precipitation changes vary among models; normally the smallest change occurs under B1 scenario, and the highest under A2 scenario. For example, the smallest decrease occurs under B1 scenario, and the largest decrease occurs under A2 scenario for the GFDL-derived precipitation change in the 21$^{st}$ Century (Fig 4). The simulations showing decreased precipitation include: GFDL simulation under B1 scenario, UKMO simulation under B1 scenario, GFDL simulation under A1B scenario, GFDL simulation under A2 scenario, and UKMO simulation under A2 scenario.

Figure 5 and figure 6 show the spatial patterns of multi-model averaged changes in precipitation and temperature across the SUS under three climate scenarios. The projected changes in precipitation and temperature varied substantially across the SUS. The precipitation mainly increases in northwestern and northeastern portions while decreases in the southwestern portions of the SUS from the 2000s to the 2050s under all three climate scenarios. From the 2050s to the 2090s, the precipitation increases occur in the northeastern portions, while decreases in the western portions of the SUS under the A1B and B1 scenarios and south under the A2 scenario. The projected temperature dramatically increases from the 2000s to the 2050s, and then slightly increases from the 2050s to the 2090s. From the 2000s to the 2050s, the temperature increase shows a gradient, with the increasing rate decreasing from the west to the east (Fig 5). The highest increase is > 5°C/century (Fig 6B, 6D, and 6F), which is expected to generate substantial impacts on ecosystem functioning such as carbon and water fluxes.

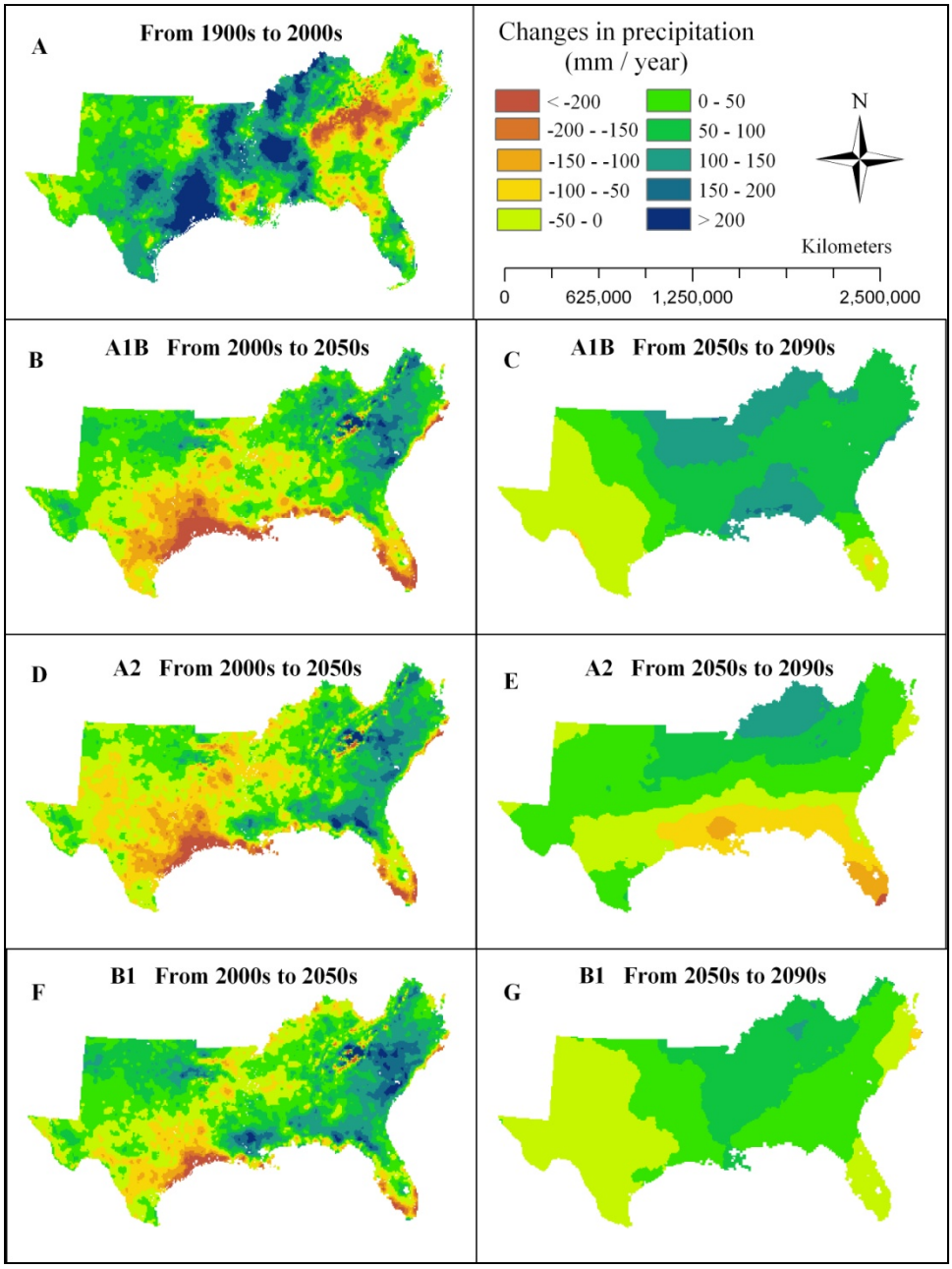


Figure 5 Spatial variations of multi-model averaged changes in precipitation over the study period (A: changes of precipitation from the 1900s to the 2000s; B: changes of precipitation under A1B scenario from the 2000s to the 2050s; C: changes of precipitation under A1B scenario from the 2050s to the 2090s; D: changes of precipitation under A2 scenario from the 2000s to the 2050s; E: changes of precipitation under A2 scenario from the 2050s to the 2090s F: changes of precipitation under B1 scenario from the 2000s to the 2050s; G: changes of precipitation under B1 scenario from the 2050s to the 2090s)

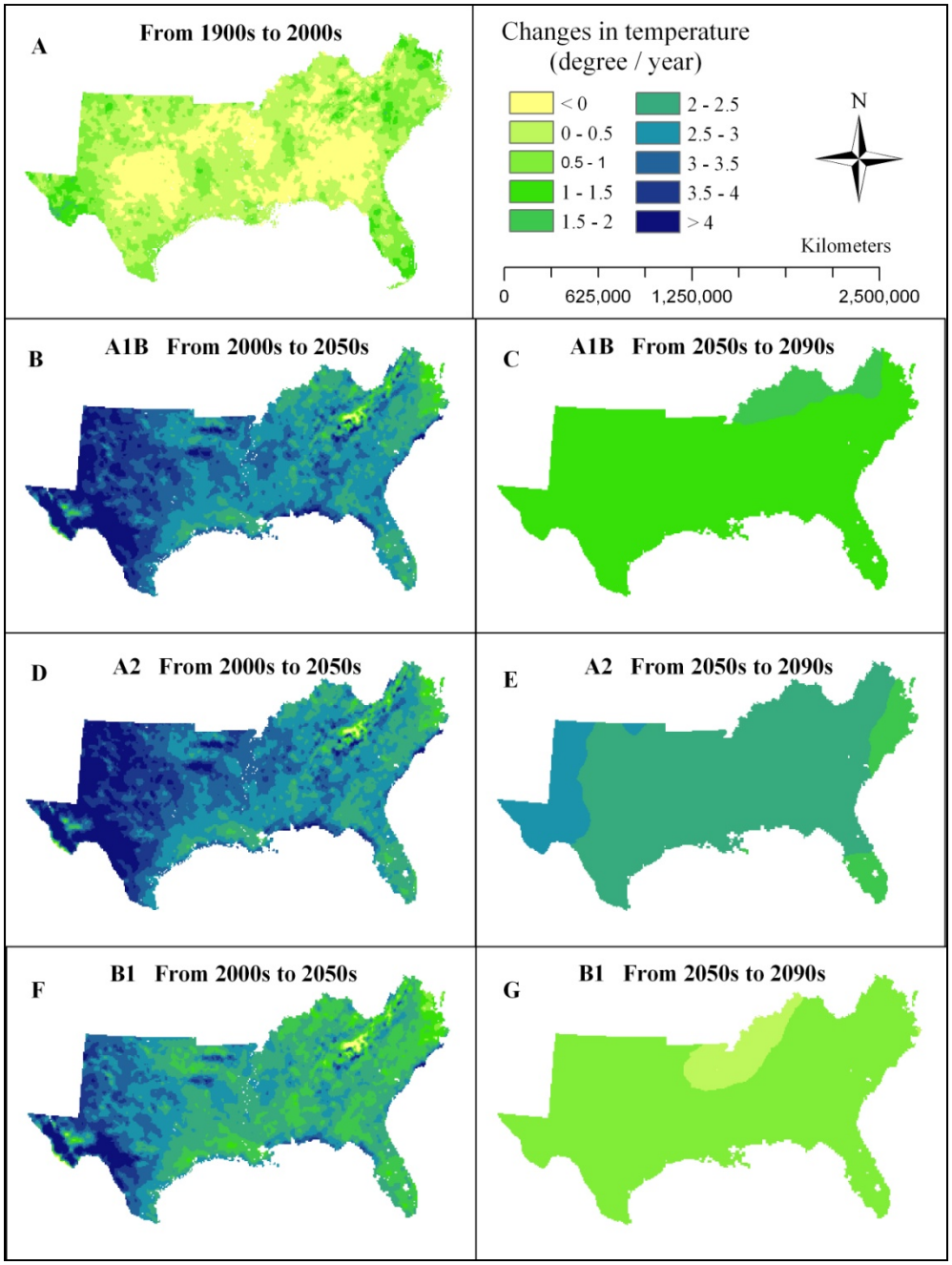


Figure 6 Spatial variations of multi-model averaged changes in temperature over the study period (A: changes of temperature from the 1900s to the 2000s; B: changes of temperature under A1B scenario from the 2000s to the 2050s; C: changes of temperature under A1B scenario from the 2050s to the 2090s; D: changes of temperature under A2 scenario from the 2000s to the 2050s; E: changes of temperature under A2 scenario from the 2050s to the 2090s F: changes of temperature under B1 scenario from the 2000s to the 2050s; G: changes of temperature under B1 scenario from the 2050s to the 2090s)

*2.3.2 Land Use/Cover Change (LULC) Data*

For the historical simulations, the same land use data utilized in Chen et al. (2006) and Zhang et al. (2008) were used in this study. The contemporary land-use map derived from the USGS National Land Cover Datasets (http://edc.usgs.gov/products/landcover.html) was combined with the historical census datasets of croplands, urban area, and population to reconstruct the annual maps of cropland and urban/developed regions from 1895 to 2007. Firstly, the 30-m resolution National Land Cover Map from USGS was aggregated into 8 km resolution and the fraction of human disturbed land-cover types (cropland and urban/developed region) in each grid was estimated. Then for the cropland data, temporal interpolation was done by calculating the cropland percentage for each cell in each year based on the cropland census data (Waisanen and Bliss, 2002) as the changing trends. In this study, county-level relative change of cropland from the Census of Agriculture (http://www.agcensus.usda.gov/) was used to control the total area of cropland to match the county-level data. Finally, the annual maps of cropland and urban distribution over the SUS covering the time period of 1895-2007 was generated; the land cover type was kept unchanged after 2008.

*2.3.3 $CO_2$ Data*

The DLEM uses the annual $CO_2$ concentration as input to simulate the effects of atmospheric $CO_2$. For the pre-2003 time period, the standard IPCC $CO_2$ concentration (Enting et al. 1994) was used in the simulations. Annual $CO_2$ concentration for years between 2003 and 2009 was calculated based on the "Global Annual Mean Growth Rate of $CO_2$" by Earth System Research Laboratory (ESRL, http://www.esrl.noaa.gov/gmd/ccgg/trends/). For each of the future climate scenarios, the projected atmospheric $CO_2$ concentrations for three climate scenarios used in the IPCC Fourth Assessment Report were used in this study. Due to the shortage of spatial

distribution of $CO_2$ concentration data, the evenly distributed $CO_2$ concentration across the study area is assumed and used in this study. The temporal variations of atmospheric $CO_2$ concentration under each of the three scenarios are illustrated in the Figure 7. The A2 scenario has the rapidest increase, while the B1 scenario has the slowest increase in the 21st century.

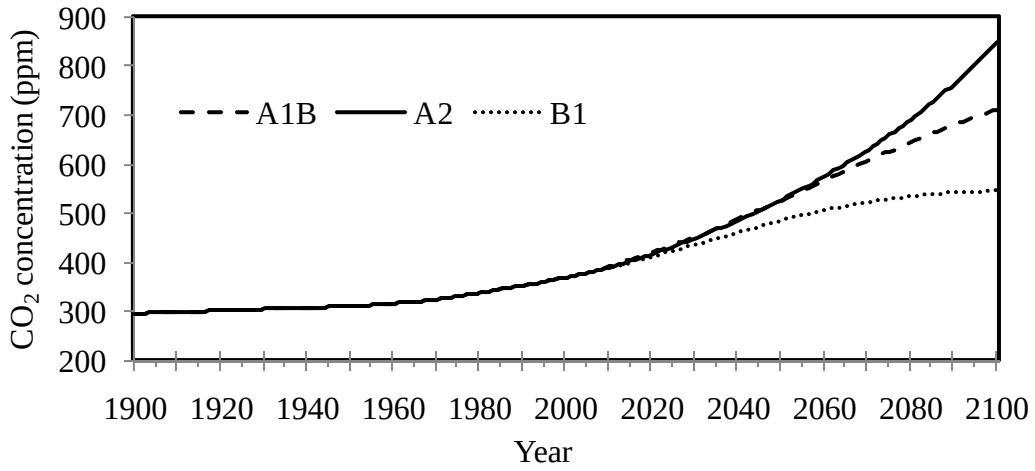


Figure 7 Temporal variations of atmospheric $CO_2$ concentration under three scenarios from 1900 to 2099

*2.3.4. Nitrogen Deposition Dataset*

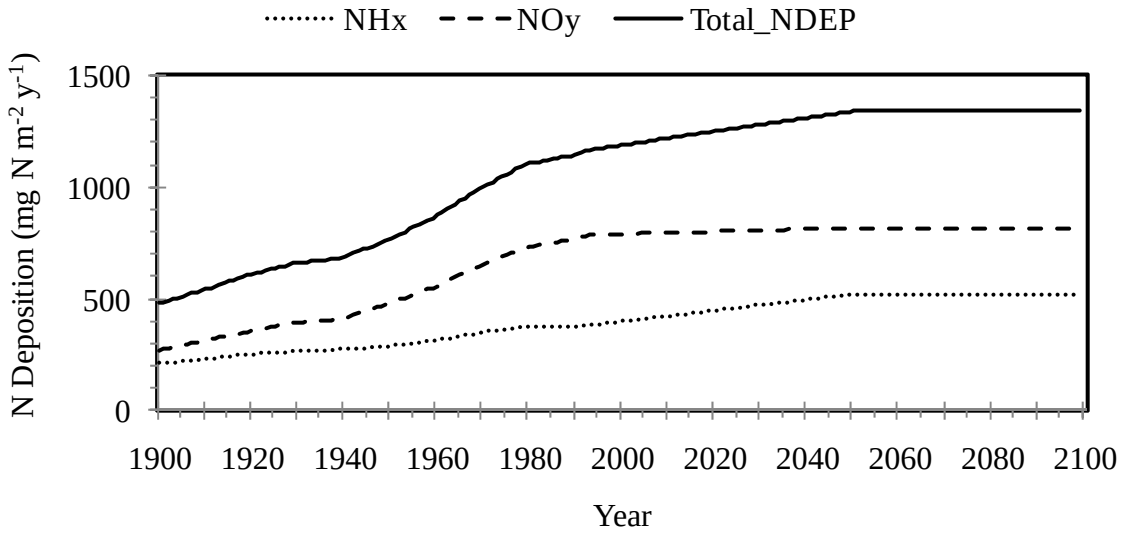


Figure 8 Temporal patterns of nitrogen deposition from 1900 to 2099 interpolated on the basis of the three period (1860, 1993, and 2050) N deposition dataset of Dentener (2006)

On the basis of Dentener's global nitrogen deposition dataset (Dentener et al., 2006), the nitrogen deposition datasets was constructed based on the three periods (1860, 1993, and 2050). The time series of gridded nitrogen deposition data at annual time step during 1860-2050 were developed from global atmospheric nitrogen deposition maps in 1860, 1993 and 2050 with a spatial resolution of 5 degrees longitude by 3.75 degrees latitude (Galloway et al., 2004; Dentener, 2006; http://daac.ornl.gov/CLIMATE/guides/global_N_deposition_maps.html). Annual variation of nitrogen deposition rate from 1890 to 1990 was controlled by EDGAR-HYDE 1.3 nitrogen emission data, which provides information on annual totals of $NH_3$ and $NO_x$ emissions from 10 anthropogenic sources within 1 × 1 degree grid cells for each decade (Van Aardenne et al., 2001; http://gcmd.nasa.gov/records/GCMD_EDGAR_HYDE.html). For this time period, it is assumed that the temporal trends of NHx-N and NOy-N deposition are consistent with those of NH3 and NOx emissions, respectively. N deposition is assumed to increase linearly over the rest of the time periods (i.e., 1860-1990 and 1990-2050). From the global nitrogen deposition dataset, the dataset for SUS region was extracted and reprojected them into 8 km resolution using bilinear interpolation. Nitrogen deposition temporal patterns are showed in Figure 8. The temporal patterns showed that before 1980, the N deposition increased more rapidly than that of post 1980. The nitrogen deposition after 2050 is assumed unchanged due to the shortage of data. Figure 9 shows the spatial distribution of nitrogen deposition in 1900, 2000, and 2099.

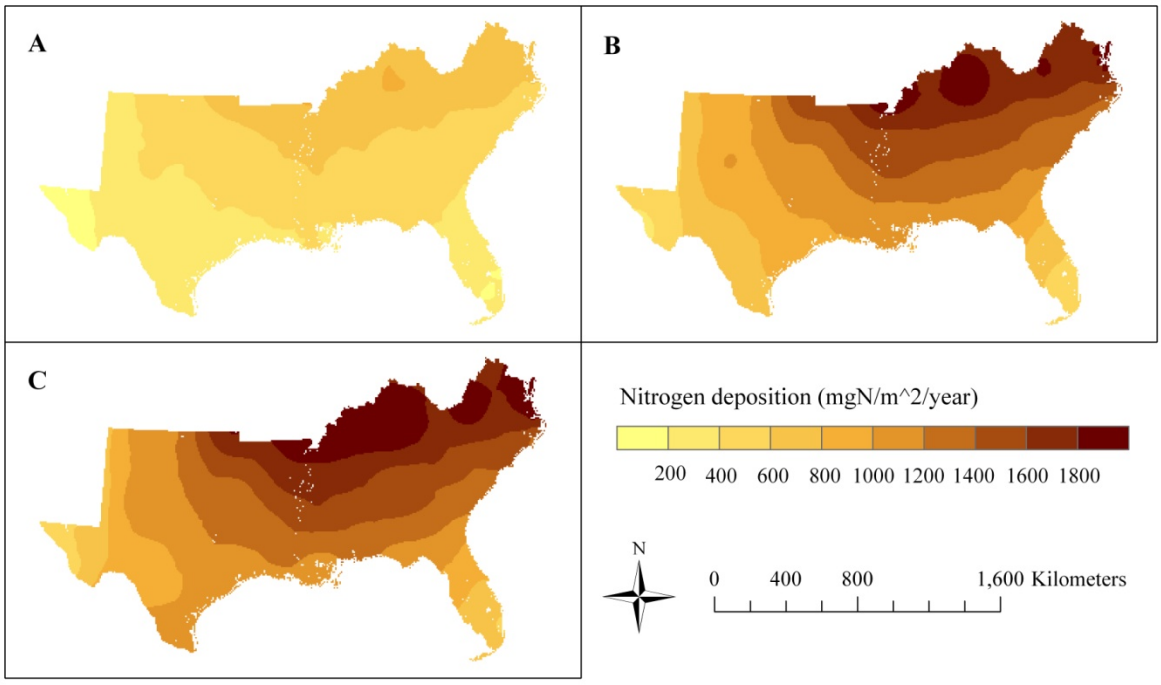


Figure 9 Nitrogen deposition in the year 1900 (A), 2000 (B), and 2099 (C) illustrated as examples

*2.3.5. Tropospheric Ozone Concentration (AOT40 index)*

The ozone effect is calculated as a function of AOT40 index in the DLEM (Ren et al., 2007). The AOT40 index is defined as the accumulated dose over a threshold of 40 ppb during daylight hours in each day (Felzer et al., 2004). For the historical dataset, a spatially explicit dataset of historical changes in the AOT40 index was developed by extracting the data from the global $O_3$ dataset developed by Felzer et al. (2004). For the future dataset (1995-2099), the AOT40 datasets was generated from the MIT-IGSM, along with the MIT-IGSM predicted climatology. For each scenario, the dataset of MIT IGSM was used to produce $O_3$ emissions from 1995-2099 and latitudinal band ozone from 1977 to 2099. Since the original global $O_3$ dataset is at monthly time step, a linear interrelation was used to get the daily $O_3$ concentration;

and the reprojection was conducted to convert original data to a spatial resolution of 8km by 8km to drive the DLEM.

Figure 10 shows the temporal pattern of the $O_3$ concentration over the study area from 1900 to 2099, while Figure 11 shows the spatial variation of $O_3$ concentration over the study area in the years of 1990 and 2090. In the early 20$^{th}$ century, the $O_3$ concentration is quite low; so the AOT40 index is zero; it continuously increases to more than 2000 ppb-h by the end of 21$^{st}$ century. There is a substantial spatial variation of $O_3$ concentration with the highest concentration in the eastern while the lowest in western portions of the SUS.

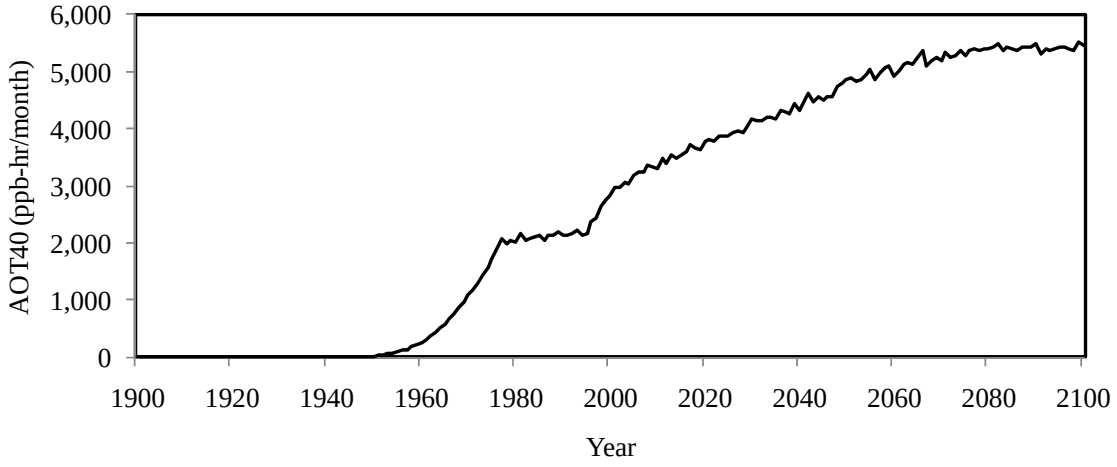


Figure 10 Temporal patterns of ozone concentration expressed AOT40 (ppb-hr/month)

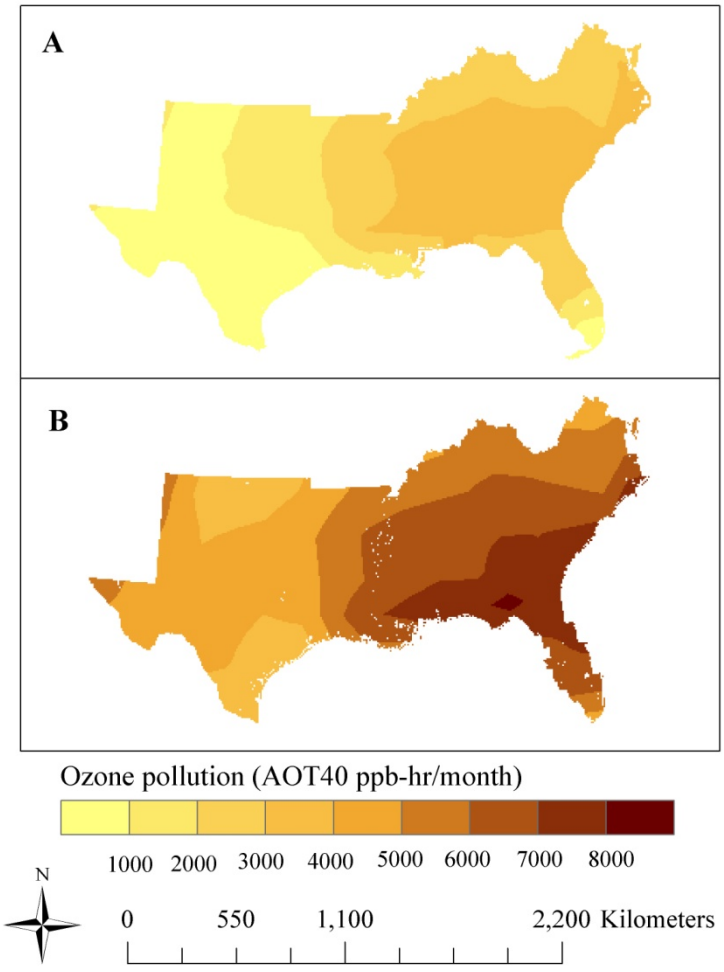


Figure 11 Spatial distribution of $O_3$ concentration in the year 1990 (A) and 2090 (B)

*2.3.6 Base Maps*

The following eleven base maps provide unchanging information of the location, topography, soil, and natural vegetation of the study region (Zhang, 2008). All of these input maps were aggregated into 8 km resolution.

(1) Elevation, slope, and aspect maps were derived from the 7.5 minute USGS National Elevation Dataset (http://edcnts12.cr.usgs.gov/ned/ned.html).

(2) Soil datasets (acidity, bulk density, soil depth (1.5 m), soil texture represented as the percentage content of clay, sand, and silt) were derived from the 1 km resolution digital general soil association map (STATSGO map) developed by the United States Department of Agriculture (USDA) Natural Resources Conservation, while the texture information of each map unit was estimated using the USDA soil texture triangle (Miller and White, 1998).

(3) The contemporary vegetation map in Figure 1 shows the distribution of four natural plant functional groups (Fig 2) of SUS before human disturbances, derived from GLC2000 with a resolution of 1 km (Bartholomé et al., 2002). The potential vegetation was reclassified into four general plant functional groups and by replacing the cropland and urban areas in the GLC2000 with the potential vegetation types from Ramankutty and Foley (1998). Water bodies were excluded from the vegetation map.

(4) The irrigation map was retrieved from global map developed by Food and Agriculture Organization (www.fao.org).

# Chapter 3 Spatial and Temporal Variations of Carbon and Water Fluxes over SUS in the Context of Multiple-Factor Global Change

## 3.1. Introduction

The carbon and water fluxes are very important processes in terrestrial ecosystems. Photosynthesis is the biological process that acts to transfer carbon from its oxidized form, $CO_2$, in the atmosphere to the reduced forms that result in plant growth (Chapin et al., 2002; Schlesinger 1997). Photosynthesis is defined as Gross Primary Production (GPP). The NPP, the abbreviation of Net Primary Production, is the net carbon sequestration by plant; it is calculated as GPP minus plant respiration. The NEP, the abbreviation of Net Ecosystem Production, is the net carbon sequestration by ecosystem; it is calculated as GPP minus ecosystem respiration including autotrophic respiration and heterotrophic respiration. The ET, the abbreviation of EvaporTranspiration, is the water released from ecosystems; it is the sum of evaporation and transpiration. The carbon gain and water use is tightly coupled through stomata (Chapin et al., 2002); the plant physiologists express the loss of water relative to photosynthesis as Water Use Efficiency (WUE) (Schlesinger 1997). Since carbon gain could be expressed at various scales, NPP at vegetation scale and NEP at ecosystem scale etc; the WUE could be defined as GPP/ET, NPP/ET, and NEP/ET etc. In this study, the NPP/ET and NEP/ET were used to show the water use efficiency in the vegetation and ecosystem perspectives.

In this chapter, the simulation with all global change factors considered was used to report the spatial and temporal patterns of carbon and water fluxes over the SUS during 1900-2099. The multi-model averaged carbon and water fluxes were reported.

### 3.2. Temporal Patterns of NPP, NEP, ET and Water Use Efficiency (WUE) during 1900-2099

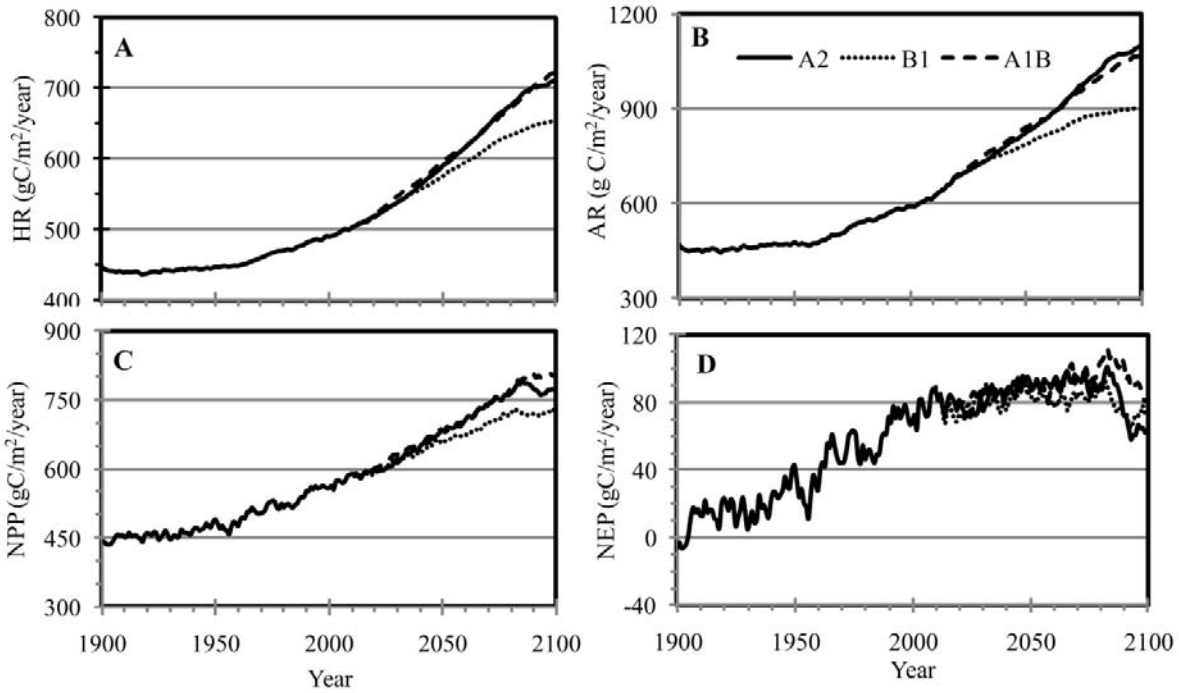


Figure 12 Temporal patterns of continental (A) HR, (B) AR, (C) NPP, and (D) NEP (HR: Heterotrophic Respiration; NPP: Net Primary Production; AR: Autotrophic Respiration; NEP: Net Ecosystem Production) considering changes of climate and atmospheric composition ($CO_2$, N deposition, and $O_3$) during 1900-2099. The results for the three different IPCC SERS-storylines (A1B, A2, and B1) with climate change projections based on four different GCMs (GFDL_CM2_1, GISS_MODEL_E_R, NCAR_CCSM3_0, and UKMO_HADCM3). The multi-model average was reported.

Figure 12 shows the 10-year running average of the carbon fluxes simulated by the DLEM over the time period of 1900-2099. For comparison purposes, the heterotrophic and autotrophic respirations were also presented. Discrepancies in carbon fluxes are observed among three climate scenarios (A1B, A2, and B1); however, the temporal patterns of HR, AR, NPP, and

NEP are similar for these scenarios. The HR, AR, NPP, and NEP show increasing trends from 1900 to 2099 (Fig 12).

The terrestrial NPP showed a continually increasing trend over the two centuries from 1900 to 2099 (Fig 12C). The average NPP over the SUS increased from approximately 457 g C $m^{-2}$ $y^{-1}$ in the 1900s, to approximately 588 g C $m^{-2}$ $y^{-1}$ in the 2000s, and approximately 766 g C $m^{-2}$ $y^{-1}$ in the 2090s.

Compared to NPP, there is more apparent inter-annual variation of net ecosystem production (NEP) (Fig 12D). Although NPP continually increases over the two centuries, it is partially canceled out by the ecosystem heterotrophic respiration (Fig 12A), especially in the 21st century. The elevated HR is probably caused by the rapidly rising temperature (Fig 3). The NEP over the SUS averaged at 16 g C $m^{-2}$ $y^{-1}$ in the first decade of the 20th century; then it increased to approximately 88 g C $m^{-2}$ $y^{-1}$ in the first decade of the 21st century, and then slightly decreases to approximately 72 g C $m^{-2}$ $y^{-1}$ in the last decade of the 21st century. The temporal pattern of NEP over the two centuries from 1900 to 2099 indicates that although the terrestrial ecosystems of SUS act as a carbon sink over the 200 years, the capacity for taking up atmospheric carbon dioxide by SUS terrestrial biosphere gradually increased during the 20th century and slightly increases in the 21st century (Fig 12D).

There is no constant changing trend in the evapotranspiration (ET) over the 200 years (Fig 13). Since 1900, ET showed an increasing trend before reaching its maximum in the 1970s; however, it decreased dramatically from the 1970s to the 2020s. By the 2020s, the ET reached its lowest over the two centuries. Although ET regains an increasing trend from the 2020s to the 2090s, the increasing rate is far less than that from the 1900s to the 1970s. Referring to the temporal patterns of temperature and precipitation (Fig 3), the dramatic decrease of ET from the

1970s to the 2020s is primarily due to the decline of temperature and precipitation during that period. Overall, the averaged terrestrial ET was approximately 708 mm for the first decade of 20th century, approximately 743 mm in the first decade of the 21st century, and approximately 731 mm in the last decade of the 21st century. Overall, there are no significant differences among climate scenarios in changing trends of carbon and water fluxes over the SUS; however, the magnitude of simulated NPP, NEP, and ET varied among climate scenarios.

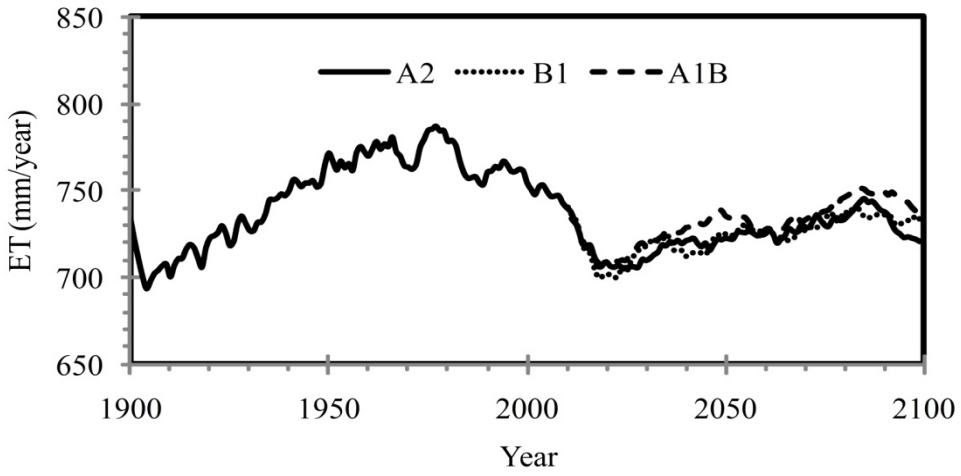


Figure 13 Temporal patterns of ET (evapotranspiration) considering changes of climate and atmospheric composition ($CO_2$, N deposition, and $O_3$) during 1900-2099. The results for the three different IPCC SERS-storylines (A1B, A2, and B1) is the average value of four different simulations with climate change projections based on four different GCMs (GFDL_CM2_1, GISS_MODEL_E_R, NCAR_CCSM3_0, and UKMO_HADCM3)

Water use efficiency (WUE) was used to quantify the coupling between carbon and water cycles and the efficiency of carbon sequestration based on water usage at ecosystem level (Yu et al., 2004; Xu and Hsiao, 2004). There are different ways to calculate WUE based on the definitions of ecosystem productions and ecosystem water fluxes (Yu et al., 2008). In this study two kinds of WUE were calculated: WUE_NPP = NPP / ET and WUE_NEP = NEP / ET (Fig 14). The terrestrial WUE_ NPP shows a slight decrease from the 1900s to the 1950s and then a continually increasing trend, ranging from 0.6 to 1.1 gC $kg^{-1}H_2O$, however, the WUE_ NEP

shows an increasing trend from the beginning of 21st century to the 2080s, and then decreases after the 2080s. The temporal patterns of WUE_NPP and WUE_NEP are quite similar to those of NPP and NEP, respectively, while are different from temporal pattern of ET. So it is concluded that the carbon fluxes control the temporal pattern of WUE, either WUE_NPP or WUE_NEP.

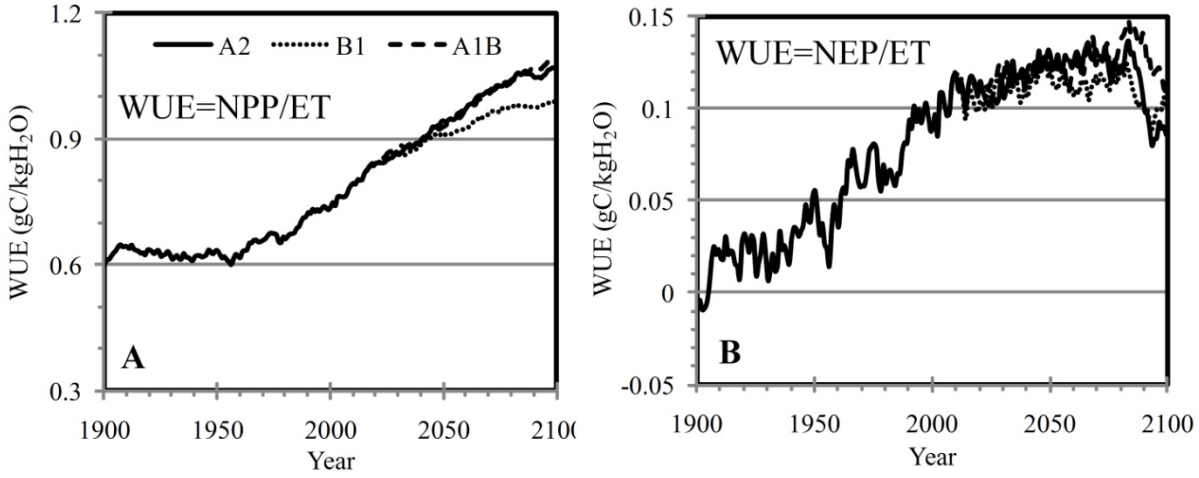


Figure 14 Temporal patterns of WUE (water use efficiency) considering changes of climate and atmospheric composition ($CO_2$, N deposition, and $O_3$) during 1900-2099. Left: WUE is the ratio of NPP to ET; Right: WUE is the ratio of NEP to ET. All the results for the three different IPCC SERS-storylines (A1B, A2, and B1) with climate change projections based on four different GCMs (GFDL_CM2_1, GISS_MODEL_E_R, NCAR_CCSM3_0, and UKMO_HADCM3; multi-model averages were reported)

### 3.3. Spatial Patterns of NPP, NEP, ET and WUE over 200 Years

The simulated NPP in eastern and central parts of SUS is far larger than that in western SUS (Fig 15). This difference is associated with vegetation distribution; the forest and woody wetland are the major contributors to the large NPP in the eastern and central portions of SUS; the small NPP in western part is mainly due to the large area of grassland, shrub and dessert. The spatial patterns of NPP over different decades show that the NPP obviously increase over 200 years from 1900 to 2099, especially from the 2000s to the 2090s. The large increase in NPP is distributed in the central and eastern portions of the SUS. The NPP increases in the west of SUS

are mainly associated with cropland distribution, since the NPP increases are scattered across the western SUS. Very similar spatial patterns of the NPP are simulated for each of three future scenarios. Under these scenarios, the uncertainties of NPP under A1B scenario is more pronounced than those under A2 and B1 scenarios, and the uncertainties under B1 scenario is smallest.

The simulated NEP shows increases across the majority of the SUS from the 1900s to the 2000s (Fig 16). Yet both increases and decreases in NEP across the SUS are observed from the 2000s to the 2090s; and the spatial patterns of NEP changes are quite different among the three climate scenarios. Under A1B and B1 scenarios, the NEP is much larger in the eastern and central portions of SUS than that in the west part; however, under A2 scenario, the NEP is quite low in the northeastern portion of the SUS. It is concluded that the capacity of carbon sequestration was enhanced during the 20$^{th}$ century across the entire region of SUS; however, this increasing trend would not continue over the 21$^{st}$ century, especially, the west part of SUS; and the NEP in the northeastern SUS will shrink. Uncertainties of simulated NEP is much larger in the northeastern and north central parts than in other regions of SUS under all three scenarios (Fig 16).

The spatial distribution of simulated ET is similar to those of NPP and NEP; large ET is mainly distributed in the eastern and central parts of the SUS (Fig 17). On the temporal scale, ET did not show an increasing trend across the entire SUS from the beginning to the end of the 21$^{st}$ century. Over the western SUS which features obvious water-limitation, the enhancement of ET in some areas is substantial due to the land conversion to cropland. For the coastal area, the ET showed an obvious decline in 2090s compared to the 2000s and the 1900s, which might is associated with the climate data. Uncertainties of ET in the future three different scenarios are

more pronounced in the western dry region, inferring the large uncertainties among climate models (GFDL, GISS, NCAR, and UKMO) (Fig 17).

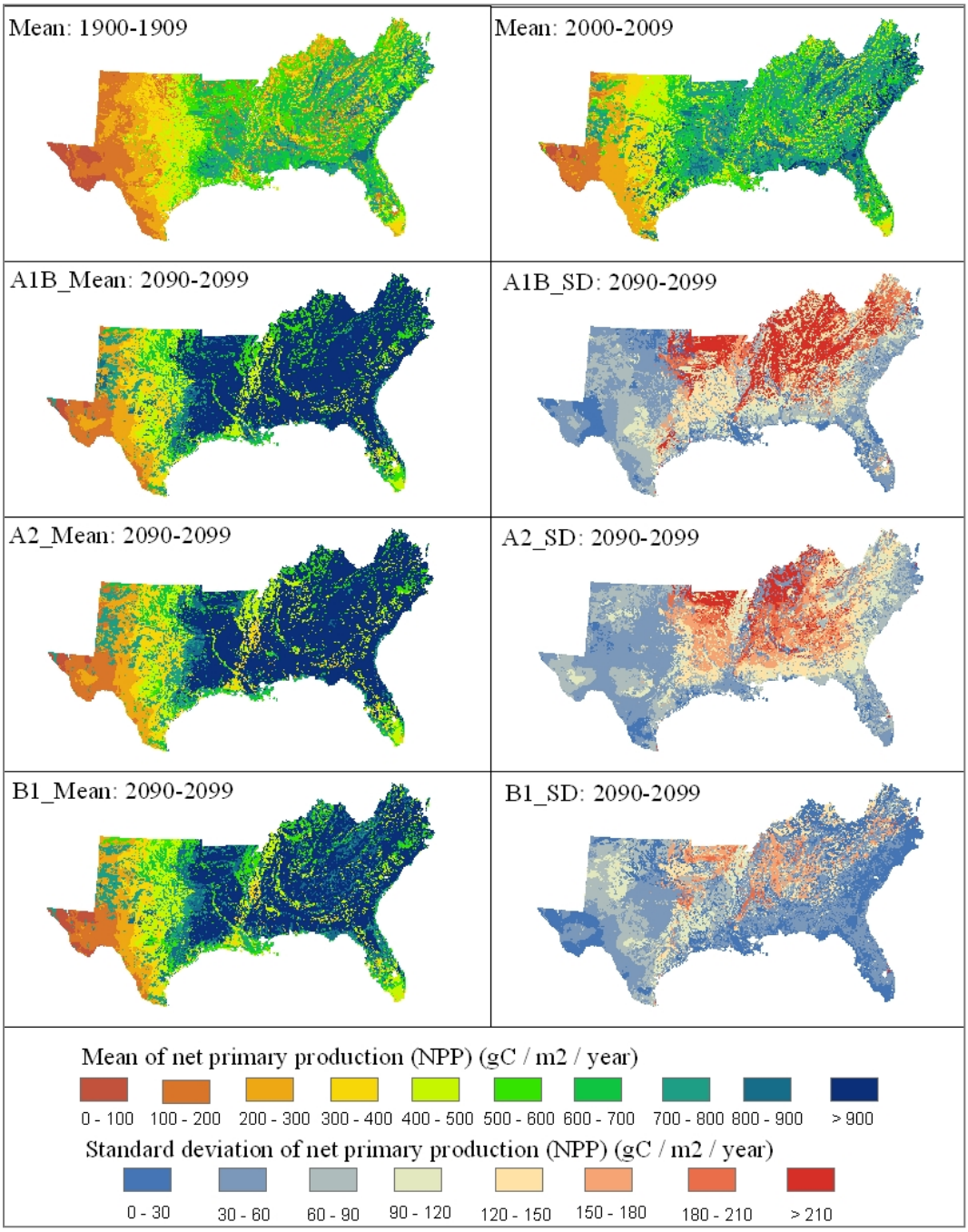


Figure 15 Spatial patterns of net primary production considering changes of climate and atmospheric composition ($CO_2$, N deposition, and $O_3$) during 1900-2099. All the future results (mean of 2090-2099) for the three different IPCC SERS-storylines (A1B, A2, and B1) with climate change projections based on four different GCMs (GFDL_CM2_1, GISS_MODEL_E_R, NCAR_CCSM3_0, and UKMO_HADCM3), the standard deviation (SD) between these models

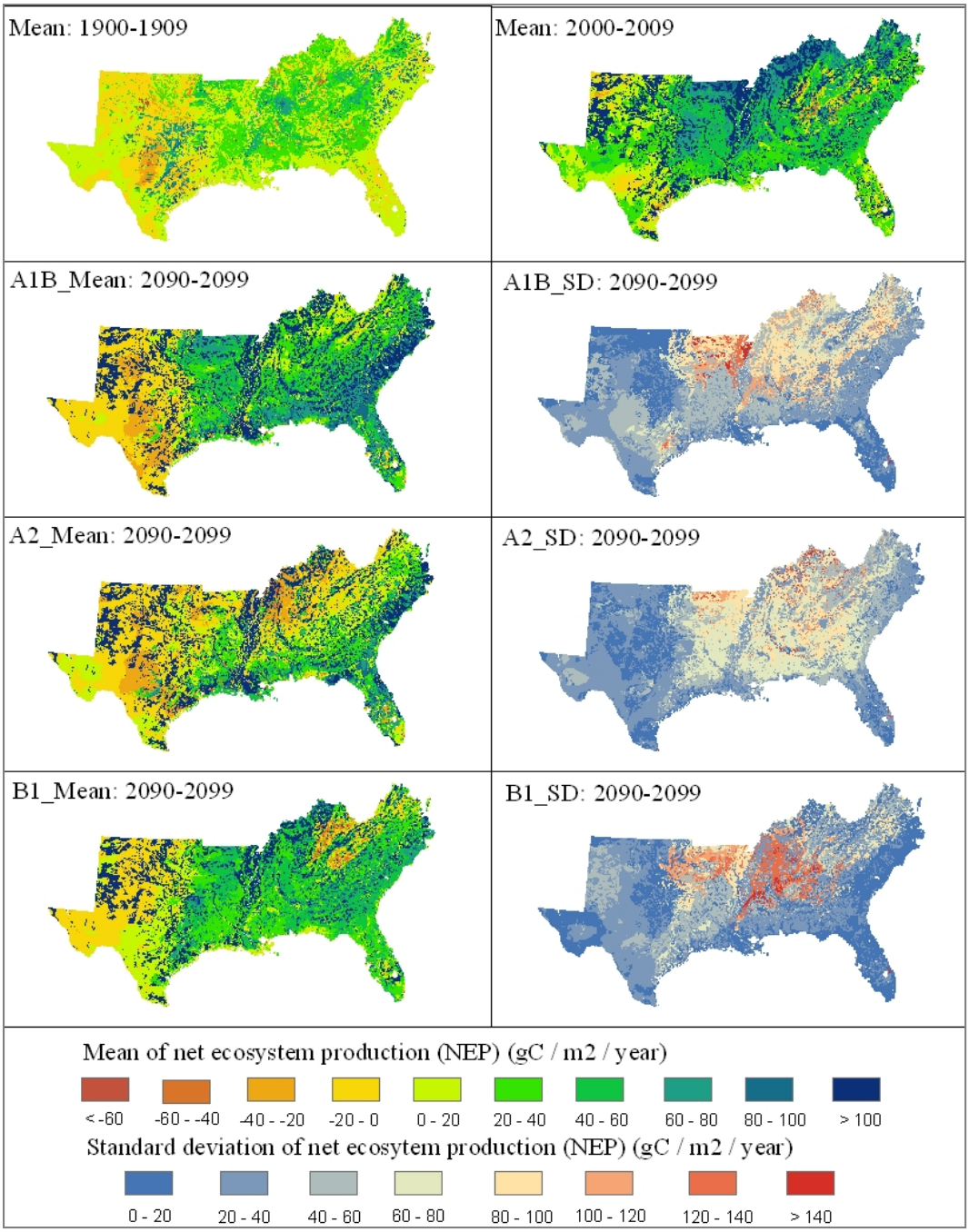


Figure 16 Spatial patterns of net ecosystem production considering changes of climate and atmospheric composition ($CO_2$, N deposition, and $O_3$) during 1900-2099. All the future results (mean of 2090-2099) for the three different IPCC SERS-storylines (A1B, A2, and B1) with climate change projections based on four different GCMs (GFDL_CM2_1, GISS_MODEL_E_R, NCAR_CCSM3_0, and UKMO_HADCM3), the standard deviation (SD) between these models

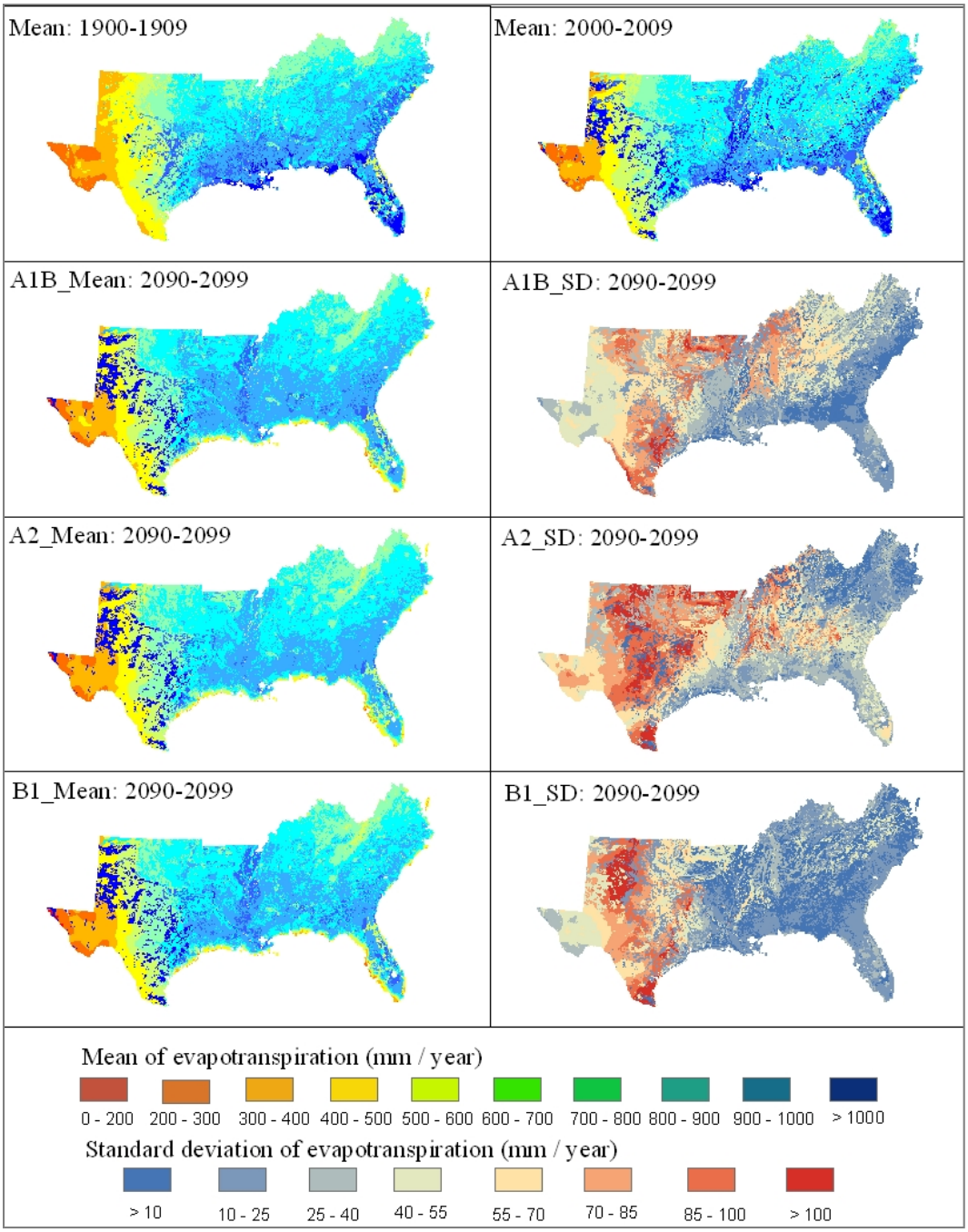


Figure 17 Spatial patterns of evapotranspriation considering changes of climate and atmospheric composition ($CO_2$, N deposition, and $O_3$) during 1900-2099. All the future results (mean of 2090-2099) for the three different IPCC SERS-storylines (A1B, A2, and B1) with climate change projections based on four different GCMs (GFDL_CM2_1, GISS_MODEL_E_R, NCAR_CCSM3_0, and UKMO_HADCM3), the standard deviation (SD) between these models

Figure 18 shows the spatial distribution of WUE_NPP for the three decades of 1900s, 2000s, and the 2090s. Over the three decades, WUE_ NPP in the central and eastern regions of SUS is much larger than that in the western SUS. In the first decade of the 20$^{th}$ century, WUE_ NPP is relatively low; large scattered spots with low WUE_NPP were observed in the central and eastern SUS; and less scattered spots of low WUE_NPP were observed in the 2000s, and much less in the 2090s. Overall, the WUE_ NPP increased substantially from the 1900s to the first decade of the 21$^{st}$ century. From the 2000s to the 2090s, no significant increase in WUE_NPP was observed; only few scattered spots in the eastern SUS shows increases in WUE_NPP. The spatial patterns of WUE_ NPP are very similar under each of the three scenarios in the 2090s. Although there is no land use information included in the future scenarios (2010-2099), the increases in WUE_ NPP across eastern and central parts of SUS by the end of the 21$^{st}$ century indicates that the nitrogen deposition, and elevated atmospheric $CO_2$ might be the enhancers for WUE_NPP. No obvious differences are observed in the spatial WUE_NPP among different climate scenarios.

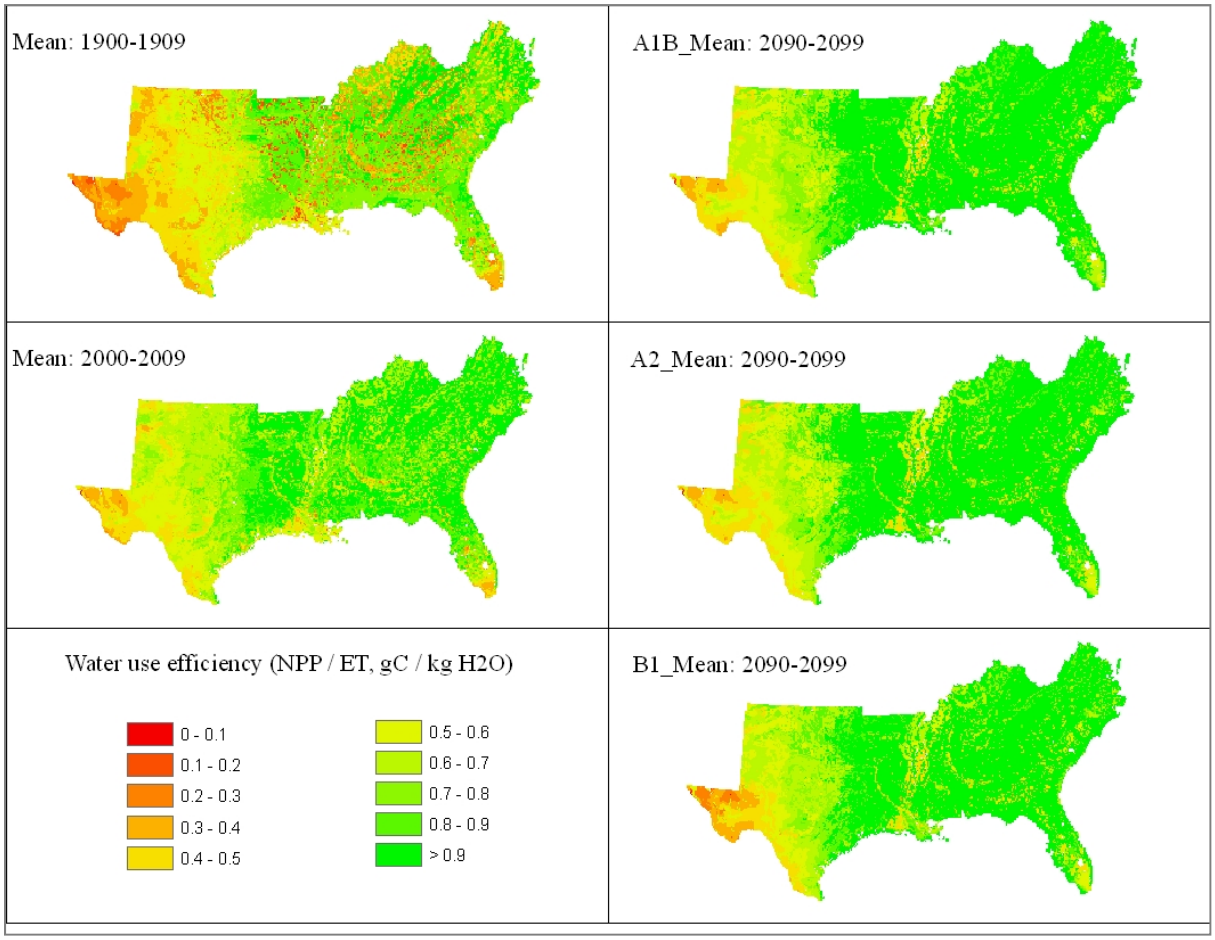


Figure 18 Spatial patterns of water use efficiency (ratio of NPP to ET, WUE_ NPP) considering changes of climate and atmospheric composition ($CO_2$, N deposition, and $O_3$) during 1900-2099. All the future results (mean of 2090-2099) for the three different IPCC SERS-storylines (A1B, A2, and B1) with climate change projections based on four different GCMs (GFDL_CM2_1, GISS_MODEL_E_R, NCAR_CCSM3_0, and UKMO_HADCM3)

WUE_ NEP could be used to estimate the magnitude of carbon fixation at the cost of one unit of water use through ET at the ecosystem level. Figure 19 shows the spatial distribution of WUE_NEP for the three decades of 1900s, 2000s, and the 2090s. In the first decade of the 20$^{th}$ century, large area of the SUS showed negative WUE_NEP which means the carbon loss at the cost of water use. There are large increases in WUE_NEP from the 1900s to the 2000s. The increases of WUE_NEP for a number of spots are distributed across the SUS. From the 2000s to the 2090s, no significant increases in WUE_NEP were observed, yet portions of the areas in the

western SUS shows decreases in WUE_NEP. In the last of the 21st century, the spatial patterns of WUE_ NEP are differing among climate scenarios, and this difference may be caused by the change of temperature and precipitation.

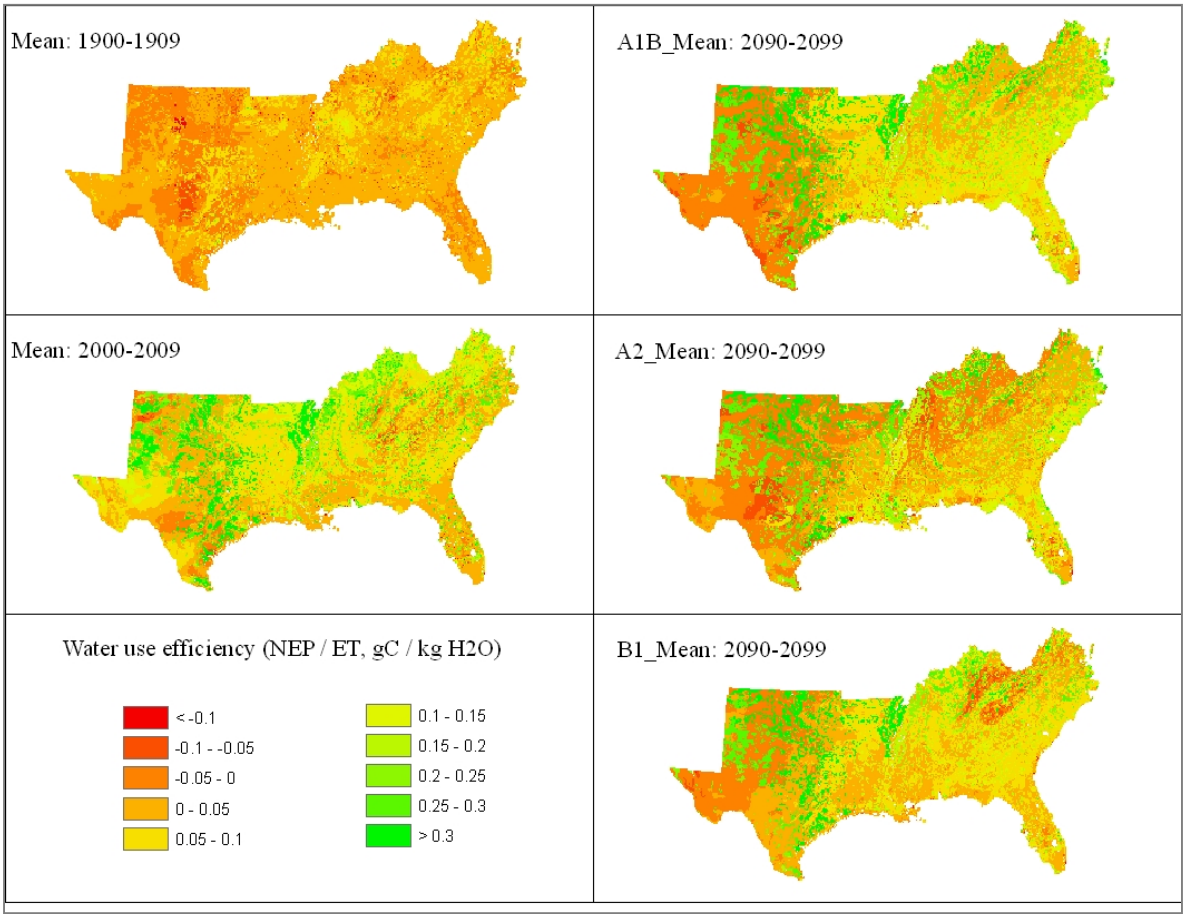


Figure 19 Spatial patterns of water use efficiency (ratio of NEP to ET, WUE_ NEP) considering changes of climate and atmospheric composition ($CO_2$, N deposition, and $O_3$) during 1900-2099. All the future results (mean of 2090-2099) for the three different IPCC SERS-storylines (A1B, A2, and B1) with climate change projections based on four different GCMs (GFDL_CM2_1, GISS_MODEL_E_R, NCAR_CCSM3_0, and UKMO_HADCM3)

### 3.4. Changes of NPP, NEP, ET, and WUE over 200 Years

In order to get a better understanding of the changes in NPP, NEP, and ET over the 200 years period, Table 3 and Figures 20-22 show the differences over time and across the space. As previously noted, the NPP continuously increases, but at a decreasing rate from the 2000s to the

2090s. NEP also increased over the 20th century, yet shows a decreasing trend over the 21st century. ET also demonstrates an increase for the first 50 years of the 20th century and a decreasing trend for the 21st century at a decreasing rate. NPP increases approximately 28.7% from the 1900s to the 2000s and increases approximately 30.4% from the 2000s to the 2090s. NEP increased approximately 434.1% from the 1900s to the 2000s; however, it decreases approximately 18.4% from the 2000s to the 2090s. ET increases approximately 4.9% from the 1900s to the 2000s, yet decreases approximately 1.7% from the 2000s to the 2090s.

Table 3 Changes of NPP (gC $m^{-2}$ $y^{-1}$), NEP (gC $m^{-2}$ $y^{-1}$), ET (mm), and WUE over 200 years

| Starting decade | | | 1900s | 1950s | 2000s | 2050s | 2090s |
|---|---|---|---|---|---|---|---|
| NPP | mean | | 456.6 | 480.7 | 587.5 | 691.8 | 766.2 |
| | | 1900s | | 5.3% | 28.7% | 51.5% | 67.8% |
| | | 1950s | | | 22.2% | 43.9% | 59.4% |
| | | 2000s | | | | 17.8% | 30.4% |
| | | 2050s | | | | | 10.8% |
| NEP | mean | | 16.4 | 32.2 | 87.8 | 85.2 | 71.6 |
| | | 1900s | | 96.2% | 434.1% | 418.8% | 335.8% |
| | | 1950s | | | 172.2% | 164.4% | 122.1% |
| | | 2000s | | | | -2.9% | -18.4% |
| | | 2050s | | | | | -16.0% |
| ET | mean | | 708.2 | 772.5 | 743.1 | 725.8 | 730.8 |
| | | 1900s | | 9.1% | 4.9% | 2.5% | 3.2% |
| | | 1950s | | | -3.8% | -6.0% | -5.4% |
| | | 2000s | | | | -2.3% | -1.7% |
| | | 2050s | | | | | 0.7% |
| WUE_NPP | mean | | 0.65 | 0.62 | 0.79 | 0.95 | 1.05 |
| | | 1900s | | -3.5% | 22.6% | 47.8% | 62.6% |
| | | 1950s | | | 27.1% | 53.2% | 68.5% |
| | | 2000s | | | | 20.6% | 32.6% |
| | | 2050s | | | | | 10.0% |
| WUE_NEP | mean | | 0.023 | 0.042 | 0.118 | 0.117 | 0.098 |
| | | 1900s | | 79.9% | 409.0% | 406.2% | 321.9% |
| | | 1950s | | | 183.0% | 181.4% | 134.6% |
| | | 2000s | | | | -0.6% | -17.1% |
| | | 2050s | | | | | -16.6% |

NPP-derived WUE shows a little decrease from the 1900s to the 1950s and then continuously increases to the 2090s; it increases 22.6% from the 1900s to the 2000s, and 32.6% from the 2000s to the 2090s. NEP-derived WUE continuously increases from the 1900s to the 2000s and then decreases to the 2090s. Over the time period of 1900s - 2000s, the NEP-derived WUE increases 409.0%, from 0.023 $gC/kgH_2O$ to 0.118 $gC/kgH_2O$, and decreases 17.1%, from 0.118 $gC/kgH_2O$ in the 2000s to 0.098 $gC/kgH_2O$ in the 2090s.

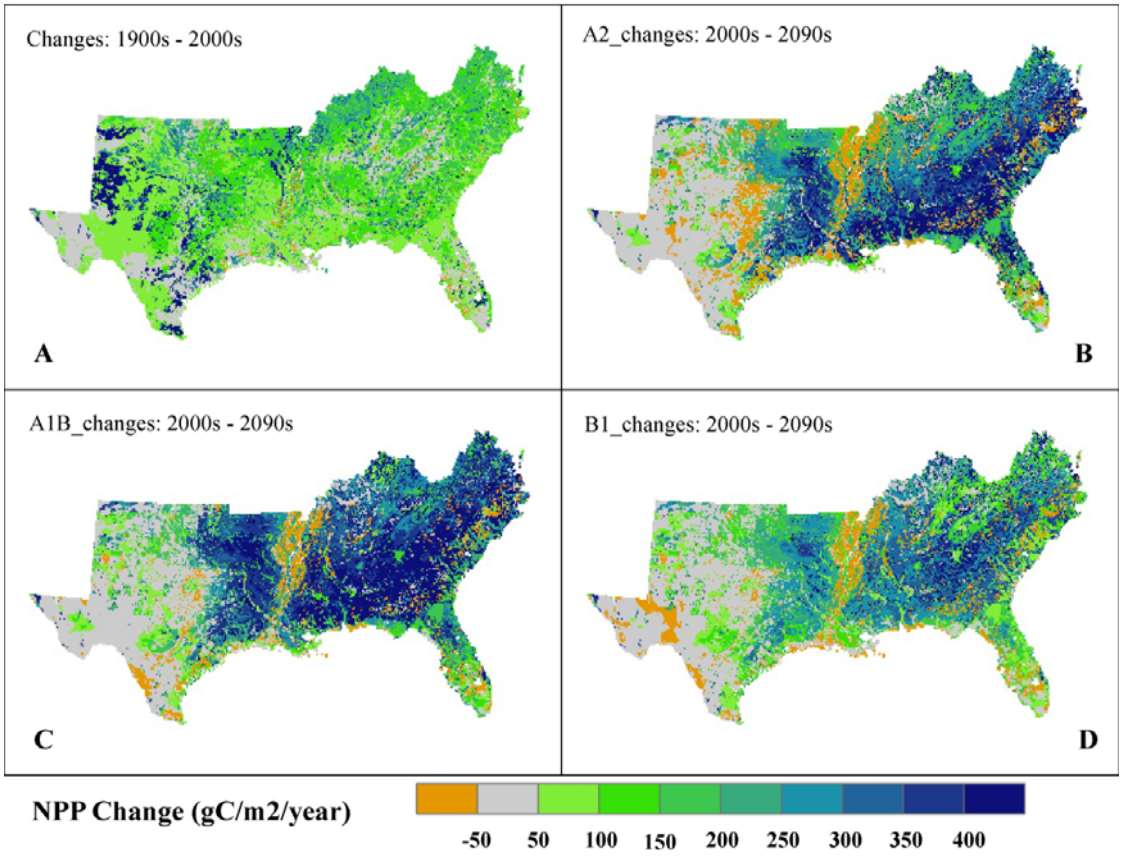


Figure 20 Spatial patterns of simulated NPP changes considering changes in climate and atmospheric composition ($CO_2$, N deposition and $O_3$) during 1900-2099. All the future results (mean of 2090-2099) for the three different IPCC SERS-storylines (A1B, A2, and B1) with climate change projections based on four different GCMs (GFDL_CM2_1, GISS_MODEL_E_R, NCAR_CCSM3_0, and UKMO_HADCM3)

The spatial pattern of NPP changes over the 20$^{th}$ century and the 21$^{st}$ century are shown in Figure 20. From the 1900s to the 2000s, medium increases in NPP were observed across the

SUS. From the 2000s to the 2090s, the increases in NPP mainly distribute in central and eastern SUS, while large portions of the western SUS show no changes in NPP. There are big differences in the simulated NPP changes over the time period of 2010-2099 among three scenarios. A1B scenario shows large area of NPP increases > 300 in the central and eastern SUS. While the B1 scenario simulates NPP increases > 100 in large portions of the central and eastern SUS. Even though large area shows simulated increases in NPP across the central and eastern SUS, small area in the central SUS showed decreases in simulated NPP.

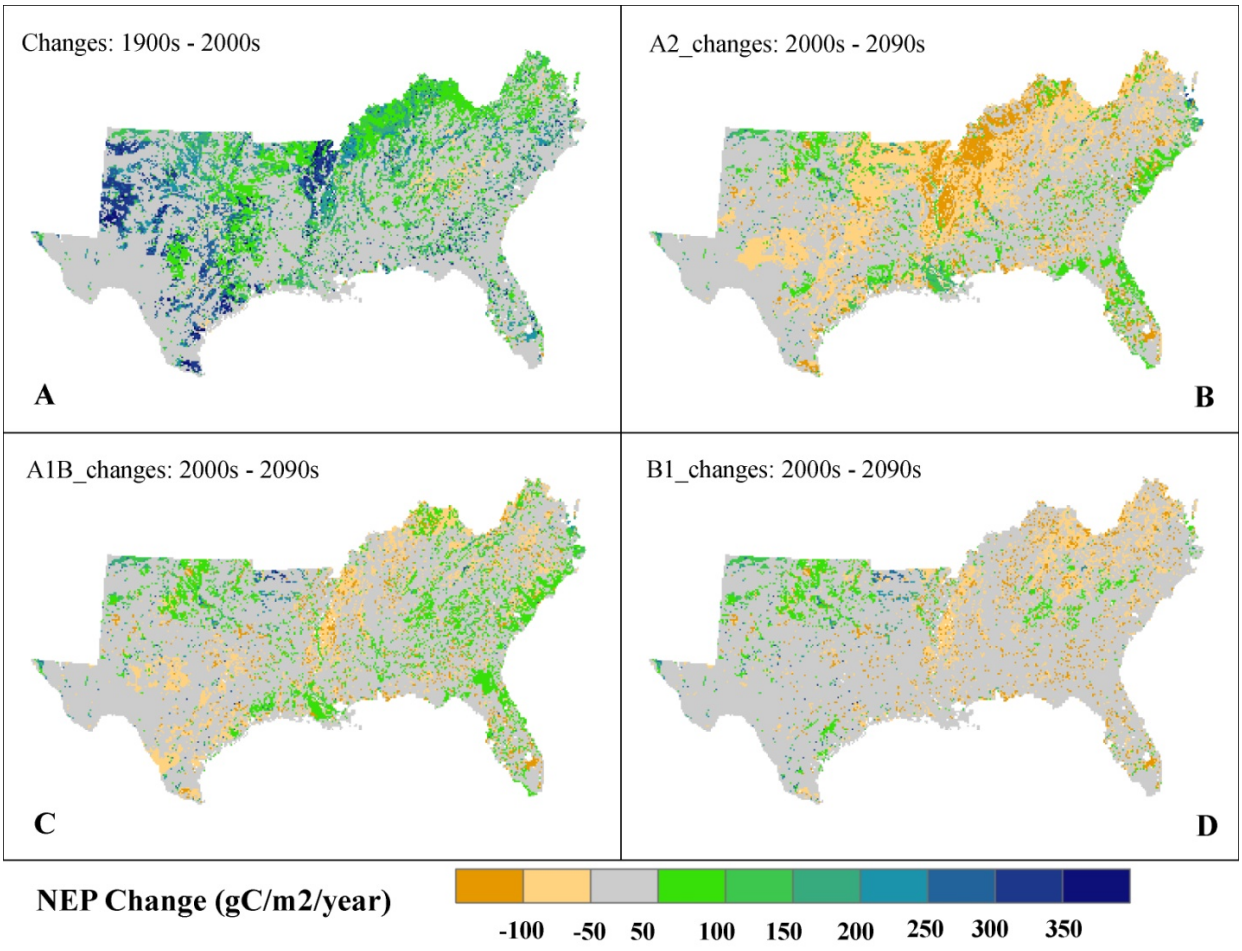


Figure 21 Spatial patterns of NEP changes considering changes of climate and atmospheric composition ($CO_2$, N deposition, and $O_3$) during 1900-2099. All the future results (mean of 2090-2099) for the three different IPCC SERS-storylines (A1B, A2, and B1) with climate change projections based on four different GCMs (GFDL_CM2_1, GISS_MODEL_E_R, NCAR_CCSM3_0, and UKMO_HADCM3)

The spatial pattern of NEP changes over the 20th century and the 21st century are shown in Figure 21. From the 1900s to the 2000s, large areas of SUS experienced increases in NEP, especially in the western SUS. From the 2000s to the 2090s, the decreases in NEP are mainly distributed in the central SUS, while large portions of the western SUS show no changes in NEP and small areas show small increases in the NEP. There are big differences in the simulated NEP changes over the time period of 2010-2099 among the three scenarios. A2 scenario shows large areas of NEP decreases > 100 in the central SUS. While the B1 and A1B scenarios simulates NEP decreases > 50 in small portions of the central SUS.

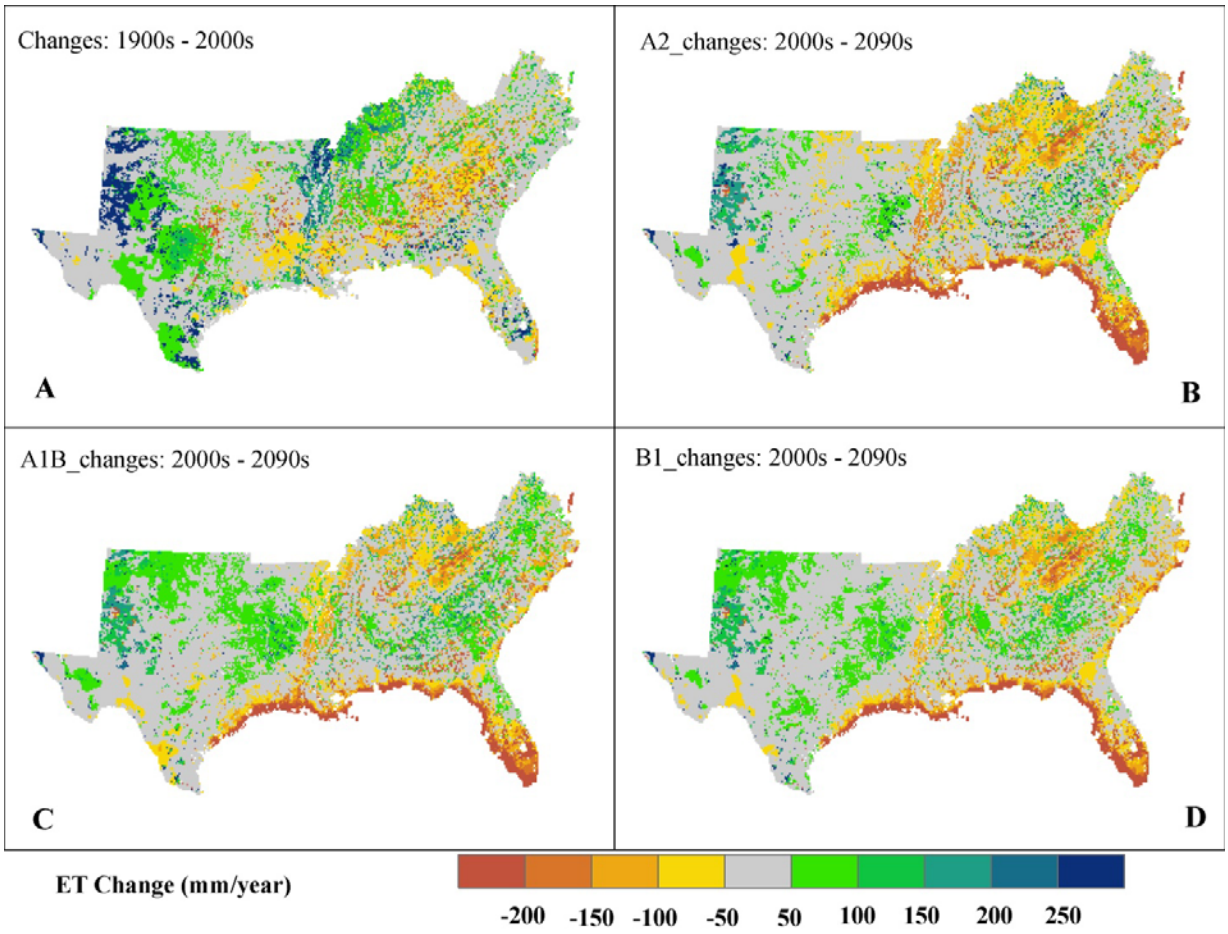


Figure 22 Spatial patterns of ET changes considering changes of climate and atmospheric composition ($CO_2$, N deposition, and $O_3$) during 1900-2099. All the future results (mean of 2090-2099) for the three different IPCC SERS-storylines (A1B, A2, and B1) with climate change projections based on four different GCMs (GFDL_CM2_1, GISS_MODEL_E_R, NCAR_CCSM3_0, and UKMO_HADCM3)

The spatial pattern of ET changes over the 20th century and the 21st century are shown in Figure 22. From the 1900s to the 2000s, medium increases in NPP were observed across the SUS. From the 2000s to the 2090s, the increases in ET mainly distribute in central and western SUS, while large portions of SUS show no changes in ET. There are no big differences in the simulated ET changes over the time period of 2010-2099 among the three scenarios. Decreases in ET are simulated in central, northeastern, and coastal area of the SUS; while the northeastern part of SUS show increases in simulated ET.

### 3.5. Factorial Contributions to the Accumulated Changes of NPP, NEP, and ET in the SUS From 2010 Through 2099

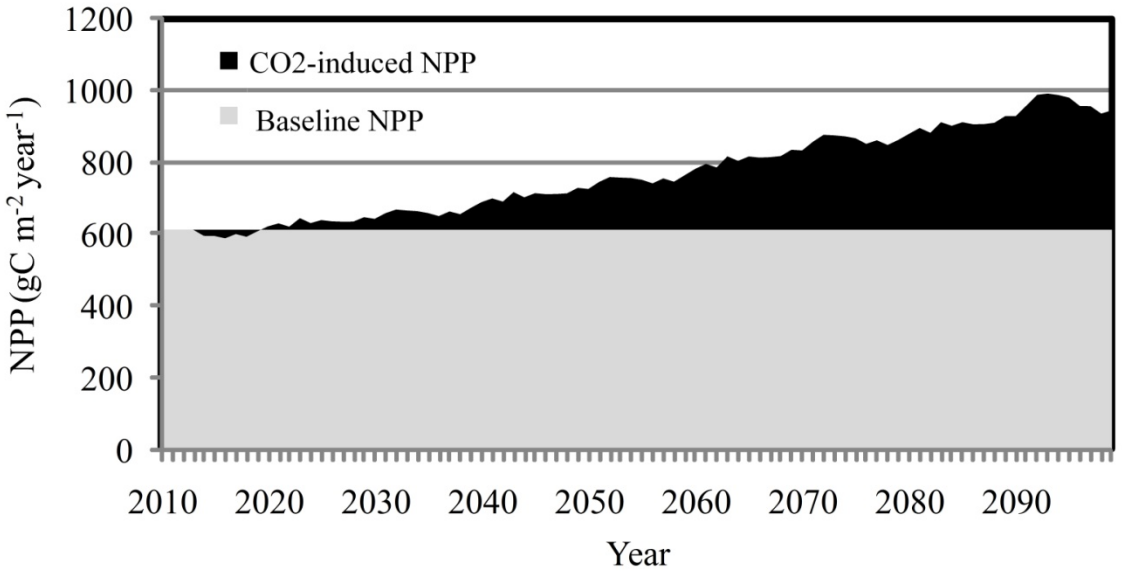


Figure 23 Diagram showing the calculation of baseline and factor-induced NPP change (The A1B scenario is used as an example to show the elevated atmospheric $CO_2$-induced NPP; the grey color shows the baseline NPP even no change of environmental factor considered, while the black color shows the NPP induced by elevated atmospheric $CO_2$ over time period; variations of simulated NPP is caused by internal system dynamic)

In order to examine the effects from different factors on NPP, NEP, and ET for the future 90 years, factorial effects were estimated by using the methodology similar to a previous study (Xu et al., 2010). The annual carbon and water fluxes in 2010 were set as the baseline, the changes in fluxes compared to the year 2010 were considered as the factorial effects. Figure 23 serves as an example to show how the effect of elevated atmospheric $CO_2$ on NPP was calculated. To quantify the factorial contributions to the variations of NPP, NEP, and ET during 2010–2099, the different single factor-induced NPP, NEP, and ET changes were calculated by subtracting annual NPP, NEP, and ET from the baseline fluxes, and then summed over the 90 years period. The interactive effect among multiple global change factors was calculated by subtracting simulated fluxes due to all factors simultaneously minus the simulated fluxes due to each single factor (Eq. 1).

$$F_{Interaction} = F_{All} - \sum F_{single} \qquad \text{Eq. 1}$$

where $F_{interaction}$ is the interactive effects of NPP, NEP, and ET caused by multiple global change factors, $F_{all}$ is the simulated fluxes induced by all environmental factors together, and $F_{single}$ is the simulated fluxes induced by each single factor such as elevated atmospheric $CO_2$, nitrogen deposition, climate change, and ozone pollution. So the interactive effect defined in this study represents the interactive effect caused by all combinations of factors including all two, three, and four factor interactions. The accumulative fluxes over the time period were calculated to quantify the factorial contributions to the carbon and water fluxes across the study area.

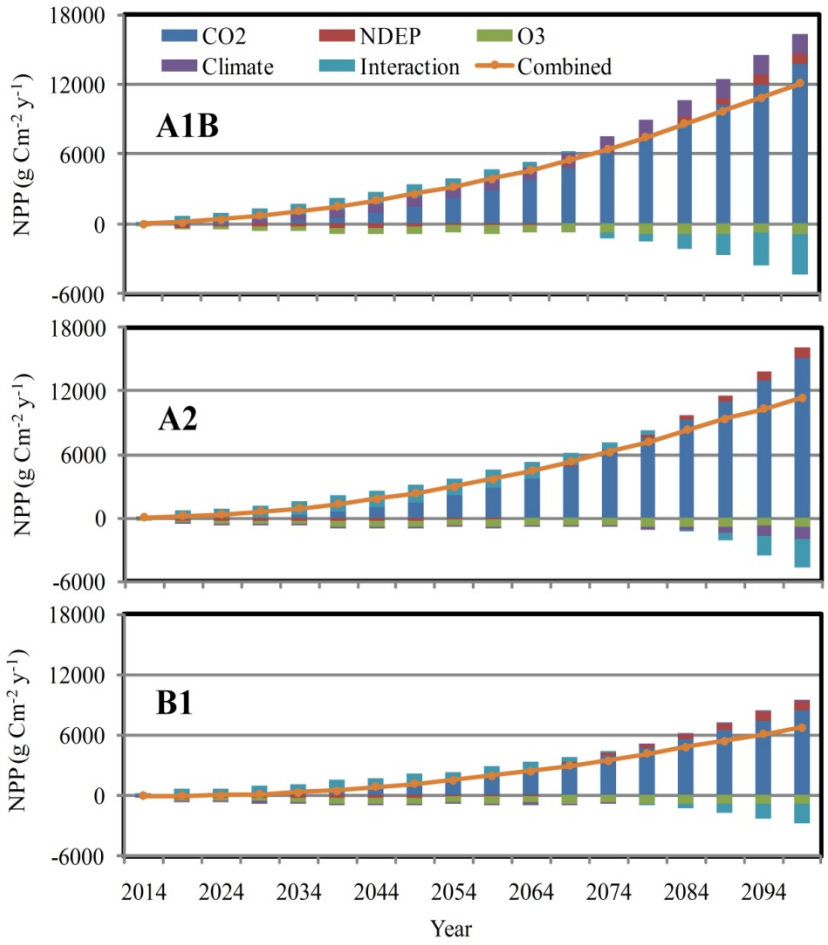


Figure 24 Factorial contributions to accumulated NPP (5-year average) in SUS during 2010–2099 (interaction means contribution from multiple-factor interaction; $CO_2$ means contribution from elevated atmospheric $CO_2$; NDEP means contribution from N deposition; $O_3$ means contribution from $O_3$ pollution; climate means contribution from climate variability)

Over the 90-year study period, various factors exerted different effects on NPP, NEP, and ET (Figs 23, 24, and 25 and Table 4). Under the three different climate scenarios, each individual factor generated similar effects on all variables yet in slightly different magnitudes. For example, climate variability yielded negative effects on NEP as simulated under three scenarios, but the magnitudes of the NEP reduction are different among scenarios. The 90-year accumulated decreases in NEP are approximately 601.80 g C $m^{-2}$ $yr^{-1}$ under A1B scenario, approximately 1804.04 g C $m^{-2}$ $yr^{-1}$ under A2 scenario, and approximately 155.47 g C $m^{-2}$ $yr^{-1}$ under B1 scenario. Overall, climate change might generate negative effects on NEP and NPP under A2

scenario, yet positive effects on ET and NPP under A1B and B1 scenarios; nitrogen deposition generated negative effects on NEP, yet positive effects on ET and NPP; elevated atmospheric $CO_2$ has positive effects on NPP and NEP, while negative effects on ET. $O_3$ brings negative effects on NPP, NEP and ET (Table 4).

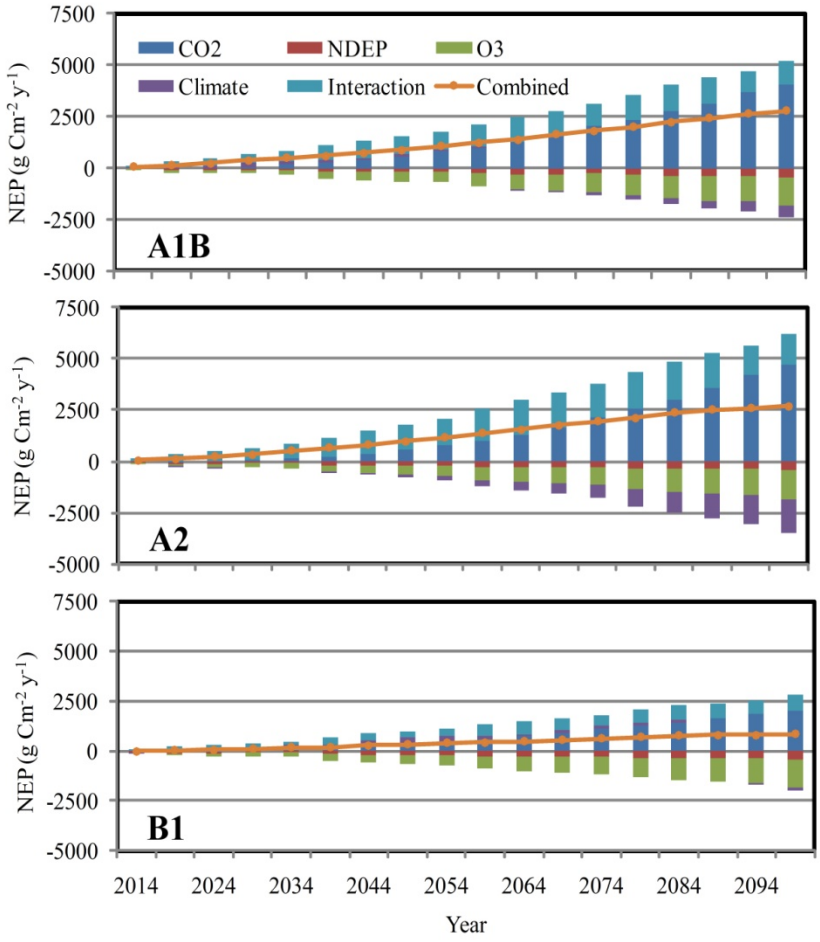


Figure 25 Factorial contributions to accumulated NEP (5-year average) in SUS during 2010–2099 (interaction means contribution from multiple-factor interaction; $CO_2$ means contribution from elevated atmospheric $CO_2$; NDEP means contribution from N deposition; $O_3$ means contribution from $O_3$ pollution; climate means contribution from climate variability)

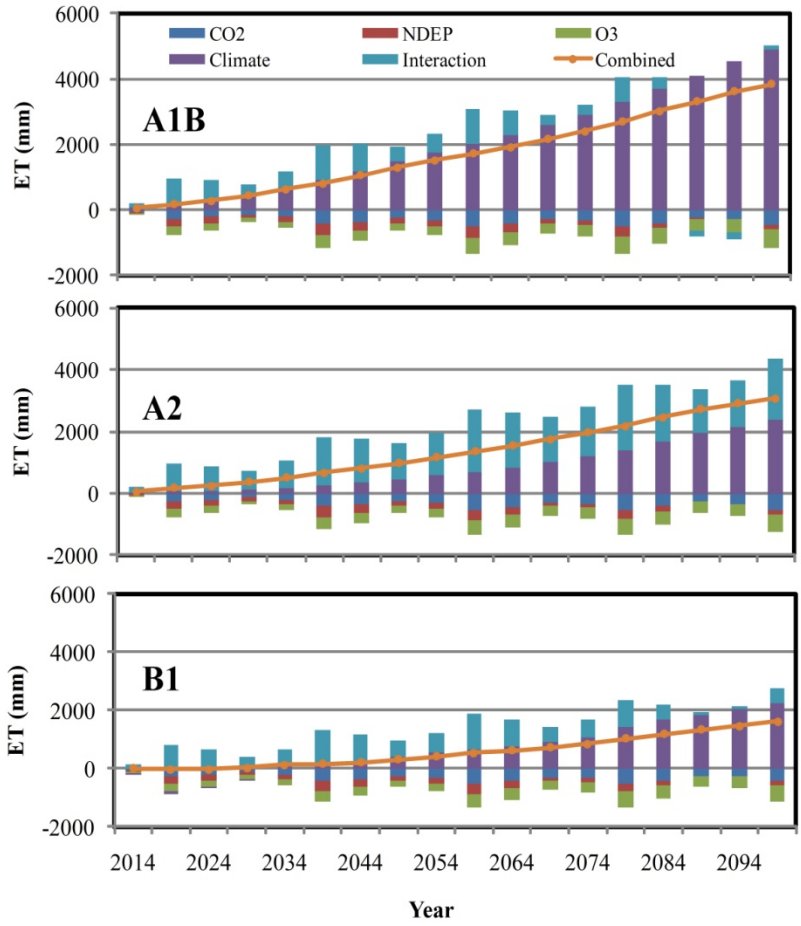


Figure 26 Factorial contributions to accumulated ET (5-year average) in SUS during 2010–2099 (interaction means contribution from multiple-factor interaction; $CO_2$ means contribution from elevated atmospheric $CO_2$; NDEP means contribution from N deposition; $O_3$ represents contribution from $O_3$ pollution; climate means contribution from climate variability)

For NPP, over the first three decades, the positive effect of $CO_2$, climate and interaction is canceled out by the negative effect of $O_3$, however, the positive effect of $CO_2$ becomes more and more pronounced and much larger than the sum of the negative effect of $O_3$ and interaction; therefore, the overall NPP shows an increasing trend in the future 90 years (Fig 24). The positive effect of $CO_2$ on NEP also becomes more and more important and much larger than the sum of the negative effect of $O_3$, climate and nitrogen deposition; therefore, NEP also presents an increasing trend in the future 90 years. For ET, climate factor and interaction generate large

positive effects. Consequently, NPP, NEP, and ET show obvious increasing trends over the time period of 2000-2099 (Figs 24 - 26).

Because water use efficiency (WUE) is a ratio of carbon flux and water flux, it is inappropriate to directly analyze the factorial contributions. Through analyzing the all combined simulation, it is concluded that $CO_2$ have positive effects on NPP and NEP, yet negative effects on ET, therefore they will have positive effect on WUE_NPP and WUE_NEP. However, the effects of climate variability, nitrogen deposition, and $O_3$ pollution on WUE depend on the magnitudes of increase or decreases of carbon and water fluxes.

Table 4 Factorial contributions to the accumulated NPP (g C $m^{-2}$ $(90yr)^{-1}$), NEP (g C $m^{-2}$ $(90yr)^{-1}$), and ET (mm $(90yr)^{-1}$) from 2010 to 2099 (Combined represents the effects with all factors being considered; Climate represents the impacts of climate variability; NDEP represents the impacts of N deposition; $CO_2$ represents the impacts of $CO_2$ variation; $O_3$ represents the impacts of $O_3$ pollution; Interaction represents all interactive effects among four environmental factors)

| | | Baseline | Climate | NDEP | $CO_2$ | $O_3$ | Interaction | Combined |
|---|---|---|---|---|---|---|---|---|
| NPP | A1B | 51260.24 | 1705.82 | 1015.60 | 14336.47 | -800.99 | -3735.17 | 12521.73 |
| | A2 | 51028.56 | -1396.42 | 1015.60 | 15938.85 | -800.99 | -2972.35 | 11784.69 |
| | B1 | 53302.19 | 100.36 | 1015.60 | 8728.69 | -800.99 | -1992.41 | 7051.25 |
| NEP | A1B | 6602.98 | -601.80 | -465.36 | 4173.52 | -1449.89 | 1188.64 | 2845.11 |
| | A2 | 6264.74 | -1804.04 | -465.36 | 4888.67 | -1449.89 | 1510.39 | 3679.77 |
| | B1 | 7744.21 | -155.47 | -465.36 | 2058.98 | -1449.89 | 865.62 | 853.88 |
| ET | A1B | 61902.77 | 3939.51 | -170.94 | -510.54 | -619.20 | 202.84 | 2841.67 |
| | A2 | 61973.23 | 3121.04 | -170.94 | -612.90 | -619.20 | 2095.89 | 3813.89 |
| | B1 | 63492.97 | 1688.47 | -170.94 | -467.37 | -619.20 | 615.74 | 1046.70 |

### 3.6. Effects of Changes in Climate and Atmospheric Composition on Carbon and Water Fluxes

Rapid and simultaneous changes in temperature, precipitation, atmospheric $CO_2$ concentration, nitrogen deposition, $O_3$ pollution are predicted to occur over the 21$^{st}$ century (Aber et al., 1995; Maurer et al., 1999; Ollinger et al., 2002; Hyvonen et al., 2007). These changes will alter carbon and water fluxes in various ecosystems; usually elevated atmospheric

$CO_2$ and increased nitrogen deposition could enhance carbon sequestration; however climate change and $O_3$ pollution normally reduce carbon sequestration (Ollinger et al., 2002; Mäkipää et al., 1999). In this study it is found that various factors generated different effects on carbon and water fluxes in SUS. Climate change and elevated atmospheric $CO_2$ are two major factors for the changes in carbon and water fluxes during 2010-2099. Heimann and Reichstein reported that many lines of evidence show that the variations in the $CO_2$ growth rate are mainly caused by terrestrial effects, in particular the impacts of heat and drought on the vegetation of western Amazonia and southeastern Asia, leading to ecosystem carbon losses through decreased vegetation productivity and/or increased respiration; furthermore, these variations not only reflect short-term responses of the carbon cycle to climate perturbations but also show the interactions between ecosystems and climate operates on timescales of millennia and longer (Heimann and Reichstein, 2008). Climate and $CO_2$ have an interactive effect on carbon flux of terrestrial ecosystem; terrestrial ecosystem is able to provide negative feedback to rising $CO_2$ and temperature until the temperature climbs so high that the stimulating effect on respiration exceeds the $CO_2$ fertilization effect (Friedlingstein et al., 2006).

The FACE experiments in a Southeastern United States hardwood forest suggests that elevated atmospheric $CO_2$ reduces transpiration rate (Wullschleger and Norby, 2001) through a reduction in stomata conductance (Lockwood, 1999). Furthermore, increase in atmospheric $CO_2$ can increase interception by increasing leaf area index (Lichter, et al., 2000). However, a experiment conducted in the Duke Forest FACE suggested that leaf area index, stomatal conductance, Ci/Ca and bulk canopy conductance are, to a first order, unaltered by elevated $CO_2$ (Ellsworth, et al., 1995; Katul et al., 2000; Pataki et al., 1998; Schäfer et al., 2002). Therefore,

the effects of elevated $CO_2$, including its shifts in the other climatic factors, on numerous factors in forest ecosystems still remains uncertain.

In addition, the simulation results from four different GCM models showed that precipitation will decrease in the future 90 years compared to current situation. Medvigy et al. pointed out that increasing variability in precipitation would lead to lower rates of carbon sequestration, and temperature variability has minor impacts (Medvigy et al., 2010). Furthermore, changes in precipitation will have direct effects on ecosystem carbon and water dynamics (Heimann and Reichstein, 2008).

In this study, it is found that both climate and $O_3$ exerted negative effects and elevated atmospheric $CO_2$ yielded a positive effect on carbon sequestration, and these phenomena are consistent with other studies (Chen et al., 2006; Ren et al., 2007; Sitch et al., 2007). This study also indicates that nitrogen deposition has a negative effect on NEP during 20010-2099; this is contrasting with other study which supports the nitrogen input could lead to more carbon sequestration (Lu 2009). This difference might be due to the higher NEP at the baseline condition in this study (Fig 13). Sing-factor responses can be easily misleading because of the interactions between factors, in particular those between N and other factors (Hyvonen et al., 2007). In addition, this study found that although all the factors of climate, $CO_2$, nitrogen deposition, and $O_3$ pollution can increases ET in the SUS over the future 90 years, the interactions among these factors decrease ET. Consequently, ET did not show an increasing trend. This also indicates that more attention should be paid to the interactions among different factor rather than the effect of single factor (Hyvonen et al., 2007).

### 3.7. Changes in Carbon and Water Fluxes under Different Scenarios

IPCC developed a set of scenarios to represent the scope of driving forces and emissions in order to reflect current understanding and knowledge about underlying uncertainties (Solomon et al., 2007). In this study three different climate change scenarios (A1B, A2, and B1) were chosen to simulate the possible changes of future temperature and precipitation conditions. Because each scenario represents unique combination of different demographic, social, economic, technological and environments, they are expected to generate distinctive effects on terrestrial fluxes of carbon and water. Temperatures tend to increase monotonically in three scenarios with different magnitude; yet there is considerable inter-decadal variability in precipitation among scenarios. All three scenarios include a period of decrease in precipitation early in the 21st. Only by combining a variety of other scenarios the potential changes of carbon fluxes could be documented. Our simulations showed that over the future 90 years, A1B scenario generated the largest NPP (23.8% larger than mean value (average value of the three scenarios) and NEP (31.2% larger than mean value), and B1 generated the smallest NPP (17.5% smaller than mean value) and NEP (28.7% smaller than mean value). The largest ET was simulated under A1B scenario (22.76% higher than mean value), and the smallest under A2 scenario (13.11% lower than mean value).

### 3.8. Uncertainties and Future Work Needs

Modeling is a powerful tool to estimate the spatial and temporal pattern of ecosystem function; yet there are many sources of uncertainties including input data, parameters, model structure, etc (Haefner 2005). This study used the improved ecosystem model, in conjunction with newly developed input data and well-calibrated parameters, to examine the spatiotemporal patterns of carbon and water fluxes across the SUS. Through this study, several aspects were

indentified for further improvements. First, the use of irrigation was simulated as an automatic process keeping soil moisture higher than permanent wilting point rather than a management practice in current study, which might result in an overestimation of WUE for croplands. Previous studies indicate that irrigation water should be quantified to accurately reflect the WUE of croplands (Howell 2001). Second, although most of model driving forces are from available data sources which have been validated, there may still be uncertainties when interpolating these data to a regional scale and reprojecting them to be consistent with model simulations. Third, the shift in vegetation types over the time period in the 21$^{st}$ century simulated by other models may have effects on results of this study (Bachelet et al., 2001, 2003). In the near future the vegetation dynamic might be an important task to improve for the DLEM model. Fourth, the ecosystem responses to external stress are normally occurring at a physiological level; yet the current ecosystem model is unable to fully represent this mechanism. For example, the elevated atmospheric $CO_2$ will stimulate carbon sequestration and the vegetation C:N ratio will widen as a response and adaptation (Rastetter et al., 1997; Luo et al., 2004). However, most of the current ecosystem models, including DLEM, are unable to simulate this physiological response (Melillo et al., 1993; Tian et al., 2010a). The incorporation of physiological response to external environmental changes would be an improvement over the current study.

Fifth, given the limited data availability, no land-use change was considered from 2004 to 2099. Therefore, the impacts on terrestrial carbon and water fluxes reported here only refer to the climate and atmospheric change. Several studies have emphasized the role of land use changes in the carbon budget and carbon flux of the United States (Chen et al., 2006). McGuire et al. (2001) simulated the effects of cropland establishment and abandonment on carbon fluxes and concluded that land-use change impacts were more significant than climatic changes in the last

century. Sixth, the input data might be another source of uncertainty; the future ozone pollution data, future nitrogen deposition data, and projected climate scenario are generated independently (Felzer et al., 2004, 2005; Dentener et al., 2006); yet in reality, all of them is inter-linked; for example, the nitrogen and ozone are chemically linked in the atmosphere (Schlesinger et al., 1997).

Seventh, large inherent uncertainties in GCMs might bring biases in regional estimations on carbon and water fluxes (Shackley et al., 1998; Jones et al., 2006; Katz, 2002; Kooten et al., 1997), and the strong differences in sunlight and precipitation variances among GCM models and reanalysis datasets also can introduce variability for the carbon and water fluxes (Medvigy et al., 2010). In order to reduce the uncertainties introduced by GCMs, the mean simulated results of DLEM driven by climate data derived from four different GCMs climate models were reported. The comparisons of simulated results based on climate data from four models will be essential to evaluate and reduce the uncertainties in this study.

# Chapter 4 Conclusions

This study examined the spatial and temporal variations of carbon and water fluxes and the water use efficiency over the southeastern United States in the 21st century in the context of multi-factor global change. The model results indicate that from 1900 to 2009, global change enhanced the terrestrial net primary production (NPP) and net ecosystem production (NEP) across the SUS. These increases mainly occur in the central and eastern parts of SUS. From 2010 to 2099, NPP shows a continuously increasing trend before the 2080s; and the increasing trend levels off after the 2080s. There is no constant trend for evapotranspiration (ET) over the 200 years. ET showed an increasing trend before it reached its peak in the 1970s; ET decreased dramatically from the 1970s to the 2020s and then increased to the 2080s before a small decline. For the spatial pattern, ET had no consistent increase over the entire region in the 21st century; however, for the western dry regions the increase in ET is significant and for the coastal area ET shows an obvious decline.

Both the WUE_NPP and WUE_NEP show long-term increasing trends over the 200 years even with high inter-annual variations and small decreases in WUE_NPP from 1900 to the 1950s, and decline in WUE_NEP from the 2080s to the 2090s. There are considerable spatial variations in NPP, NEP, ET, WUE_NPP, and WUE_NEP across the SUS over the study period. Various single global change factors have different effects on carbon and water fluxes over the future 90 years. Climate change could increase or decrease NPP, depending upon the future climate scenario, where NEP decreased and ET increased for all scenarios. Nitrogen deposition

increased NPP while decreased ET. Elevated atmospheric $CO_2$ was projected to increase NPP and NEP, while decreasing ET. In comparison, the multiple factors interactive effects were negative on NPP, while be positive on NEP and ET over the study period.

The projected increase in NPP and NEP under the multiple-factor global change in the 21st century is consistent with one study which considered the climate change (Cao and Woodward 1998), and another study which considered multiple global change factors (Muller et al., 2007). The climate only scenario in this study showed a decrease in carbon sequestration, on contrast to Cao and Woodward (1998), yet is consistent with regional studies in the U.S. (Hurtt et al., 2001; Bachelet et al., 2001) which concluded that the carbon sink strength over the U.S. will shrink in the 21st century. The discrepancies among studies on the carbon sequestration in the 21st century indicate the large uncertainties in current modeling studies targeting understanding future carbon processes, implying the importance of more studies on future carbon and water fluxes in the SUS. Although the overall increases in the ET over the 21st are similar to the findings of Gordon and Famiglietti (2004), they concluded a continuous increase in ET over the entire SUS. The discrepancy could be due to different spatial coverage and input data used in these two studies.

The stimulating effect of nitrogen input on carbon sequestration is consistent with a number of studies at site-level or regional scale (Lu 2009; Nadelhoffer et al., 1999). One regional analysis also revealed that the nitrogen input would increase carbon storage in forest over the US (Thomas et al., 2010). A recent literature review also summarized the ecosystem responses to nitrogen deposition through many internal processes (Hyvonen et al., 2007). The nitrogen stimulation on carbon sequestration could be explained by nitrogen limitation in these ecosystems (Lebauer and Treseder 2008; Vitousek. 1991). The nitrogen stimulation of carbon

sequestration is expressed as increased carbon storage in vegetation and soil (Hyvonen et al., 2007; Janssens et al., 2010). The nitrogen deposition was simulated decreasing ET over the SUS, while previous field studies found the nitrogen input could increase (Bucher-Wallin et al., 2000) or have no significant effect (Maurer et al., 1999).

The effects of elevated atmospheric $CO_2$ on carbon and water fluxes have been studied for a long time, and the stimulating effect of elevated atmospheric $CO_2$ on carbon sequestration has been confirmed (Korner 2000; Schimel et al., 2000; Jackson et al., 2009; McGuire et al., 2001). This study concluded that elevated atmospheric $CO_2$ concentration will increase carbon sequestration in the SUS; this is consistent with a modeling study that was conducted by Schimel et al. (2000). However, since Schimel's study did not consider the progressive nitrogen limitation on $CO_2$ fertilization, their study could overestimate the carbon sink in the SUS. Mechanically, the elevated $CO_2$ concentration leads to a reduction of transpiration, thus the decreases of ET (Chapin et al., 2002; Maurer et al., 1999). Yet Korner (2000) concluded that small increases in $CO_2$ concentration would lead to small reductions of ET (Korner 2000). In this study, the simulated results confirmed the reduction of ET in response to elevated atmospheric $CO_2$ concentration, yet with considerable variations (Fig. 26).

This study concluded that the ozone pollution would have negative effects on carbon sequestration and ET across the SUS, which is consistent with field observations (Bernacchi et al., 2011; Massman and Grant 1995) and modeling studies (Felzer et al., 2004, 2005). Eventually, this study also concluded that the multiple-factor experiments could be very important tools to reveal the mechanisms for ecosystem response to environmental changes which could be used to improve regional modeling studies targeting a better understanding of the Earth system (Norby and Luo 2004).

This study is among the first attempts to examine the spatiotemporal variations of carbon and water fluxes over the SUS in the 21st century. Although uncertainties were brought in through several processes, this study has a number of implications for the scientific community, the public, and policy makers. First, this study will improve the understanding of both the public and scientific community on the trajectories of carbon and water fluxes in the 21st century, which will be helpful for the implementation of some regulations for environmental protection and the mitigation of global change. For example, the conclusion that severe ozone pollution will reduce carbon sequestration and water fluxes of the terrestrial ecosystems should encourage the public and policy makers to cooperate to reduce ozone release to the atmosphere (Bernacchi et al., 2011). Second, the spatial distribution of the changes in carbon and water fluxes over the SUS in response to the multiple factor global change will be helpful for policy maker who would like to reduce global change effects on terrestrial ecosystem at the regional scale. The area with strong effects from global change should be paid more attention, while the area with lower effect could be paid less attention. For example, the western SUS is projected to have lower changes in carbon and water fluxes in response to global change while the eastern SUS show stronger responses to global change; thus it should be more important to invest in mitigation in the eastern portions of SUS in terms of carbon and water management under the projected global change. Further, the interactive effects of multiple global change factors call for more observational and modeling study in the context of multiple-factor global change (Norby and Luo et al., 2004; Dermody 2006).

Through the comparison among simulated carbon and water fluxes by models driven by three climate scenarios, it is concluded that a balance across fossil intensive and non-fossil energy sources will be the best option to form a future world of very rapid economic growth,

global population that peaks in mid-century and declines thereafter, and the rapid introduction of new and more efficient technologies.

References

Aber, J. D., Ollinger, S. V., Federer C. A., et al. 1995. Predicting the effects of climate change on water yield and forest production in the northeastern United States. *Climate Research*, 5, 207-222.

Aber, J. D., Ollinger, S. V., Driscoll, C. T. 1997. Modeling nitrogen saturation in forest ecosystems in response to land use and atmospheric deposition. *Ecol. Model*., 101, 61–78.

Bachelet, D., Neilson, R.P., Lenihan, J.M., Drapek, R.J., 2001. Vegetation distribution and carbon budget in the United States. *Ecosystems* 4 164-185.

Bachelet, D., Neilson, R. P., Hickler, T., et al. 2003. Simulating past and future dynamics of natural ecosystems in the United States. *Global Biogeochemical Cycles*, 17, 1045, doi:10.1029/2001GB001508.

Baldocchi, D., Falge, Eva., Gu, L., et al. 2001. FLUXNET: A New Tool to Study the Temporal and Spatial Variability of Ecosystem-Scale Carbon Dioxide, Water Vapor, and Energy Flux Densities. *Bulletin of the American Meteorological Society*, 82, 2415-2434.

Baldocchi, D., Valentini, R., Running, S., Oechel, W., Dahlman, R., 1996. Strategies for measuring and modelling carbon dioxide and water vapour fluxes over terrestrial ecosystems. *Global Change Biology* 2(3) 159-168.

Bartholomé, E., Belward, A.S., Achard, F. (2002) GLC2000—Global landcover mapping for the year 2000. Project status, November 2002. EUR 20524 EN. *European Commission*, JRC, Ispra, Italy.

Bernacchi C. J., Leakey D.B., Kimball B. A., Ort D. R. 2011 Growth of soybean at future tropospheric ozone concentrations decreases canopy evapotranspiration and soil water depletion. *Environmental Pollution*, 159(6), 1464-1472.

Birdsey, R., Pregitzer, K., and Lucier, A. 2006. Forest carbon management in the United States: 1600-2100. *Journal of Environmental Quality*, 35, 1461-1469.

Black, T., DenHartog, G., Neumann, H., et al. 1996. Annual cycles of water vapour and carbon dioxide fluxes in and above a boreal aspen forest. *Global Change Biology*. 2, 219-229.

Bucher-Wallin, I.K., Sonnleitner, M.A., Egli, P., Gunthardt-Goerg, M.S., Tarjan, D., Schulin, R. and Bucher, J.B. 2000. Effects of elevated $CO_2$, increased nitrogen deposition and soil on evapotranspiration and water use efficiency of spruce-beech model ecosystems. *Phyton* **40**: 49-60.

Cao, M., Woodward, F., 1998. Dynamic responses of terrestrial ecosystem carbon cycling to global climate change. *Nature* 393(6682) 249-252.

Ciais, P., Reichstein, M., Viovy, N., et al. 2005. Europe-wide reduction in primary productivity caused by the heat and drought in 2003. *Nature*, 437, 529-533.

Chapin, F., Matson, P., Mooney, H., 2002. *Principles of terrestrial ecosystem ecology*. Springer.

Chen, H., H.Q. Tian, M. Liu, J. Melillo, S. Pan, and C. Zhang. 2006. Effects of land-cover change on terrestrial carbon dynamics in the southern USA. *Journal of Environmental Quality* 35: 1533-1547.

Cooter, E.J. 1992. General circulation models scenarios for the Southern United States. In R.A. Mickler and S. Fox (ed.) *The productivity and sustainability of Southern forest ecosystems in a changing environment*. Ecological Studies 128. Springer, New York.

Coursolle, C., Margolis, H.A., Barr, A.G., et al. 2006. Late-summer carbon fluxes from Canadian forests and peatlands along an east-west continental transect. *Canadian Journal of Forest Research* 36, 783-800.

Cox, P.M., Betts, R.A., Jones, C.D., et al. 2000. Acceleration of global warming due to carbon-cycle feedbacks in a coupled climate model. *Nature*, 408, 184-187.

Cramer W, Bondeau A, Woodward FI, et al. 2001. Global response of terrestrial ecosystem structure and function to $CO_2$ and climate change: results from six dynamic global vegetation models. *Global Change Biology* 7(4):357–73.

Dale VH., Joyce LA, Mcnulty S, Neilson RP, et al. 2001. Climate change can affect forests by altering the frequency, intensity, duration, and timing of fire, drought, introduced species, insect and pathogen outbreaks, hurricanes, windstorms, ice storms, or landslide. *BioScience*, 51, 723-734.

Denman, K.L., Brasseur, G., Chidthaisong, A., Ciais, P., Cox, P.M., Dickinson, R.E., Hauglustaine, D., Heinze, C., Holland, E., Jacob, D., Lohmann, U., Ramachandran, S., da Silva Dias, P.L., Wofsy, S.C., Zhang, X., 2007. Couplings between changes in the climate system and biogeochemistry, In: Solomon, S., Qin, D., Manning, M., Chen, Z. (Eds.), *Climate change 2007: The physical science basis. Contribution of working group I to the fouth assessment report of the intergovernmanetal panel on climate change*. Cambridge Univeristy Press: Cambridge, United Kingdom and New York, USA.

Dentener, F.J. 2006. Global Maps of Atmospheric Nitrogen Deposition, 1860, 1993, and 2050. Data set. Available on-line [http://daac.ornl.gov/; http://mercury.ornl.gov/metadata/ornldaac/html/daac/daacsti.ornl.gov_SMM_ME RCURY_harvest21_771.html] from Oak Ridge National Laboratory Distributed Active Archive Center, Oak Ridge, Tennessee, U.S.A. IPCC Special report emissions scenarios: Summary for Policymakers. 2000. Intergovernmental Panel on Climate Change. ISBN: 92-9169-113-5.

Dermody, O., 2006. Mucking through multifactor experiments; design and analysis of multifactor studies in global change research. *New Phytologist* 172(4) 598-600.

Ellsworth, D.S., Oren, R., Huang, C., et al. 1995. Leaf and canopy responses to elevated $CO_2$ in a under free-air $CO_2$ enrichment. *Oecologia,* 104, 139-46.

Enting, I.G., Wigley, T.M.L., Heimann, M. 1994 Future emissions and concentrations of carbon dioxide: key ocean/atmosphere/land analyses. CSIRO Division of Atmospheric Research Tech Paper No. 31, Melbourne.

Fang C, Smith P, Moncrieff J, Smith J. 2005. Similar response of labile and resistant organic matter pools to changes in temperature. *Nature* 433:57–58.

Felzer B.S.F., J. Reilly, J. Melillo, D. Kicklighter, C. Wang, R. Prinn, M. Sarofim and Q. Zhuang, 2003. *Past and future effects of ozone on net primary production and carbon sequestration using a global biological model*, Cambridge, MA, MIT Joint Program on the Science and Policy of Global Change, p. 42.

Felzer, B., Kicklighter, D.W., Melillo, J.M., Wang, C., Zhuang, Q., Prinn, R. 2004 Effects of Ozone on Net Primary Production and Carbon Sequestration in the Conterminous United States using a Biogeochemistry Model. *Tellus* 56B, 230-248.

Friedli H, Lotscher H, Oeschger H, Siegenthaler U, Stauffer B 1986 Ice core record of the C-13/C-12 ratio of atmospheric $CO_2$ in the past 2 centuries. *Nature,* 324, 237–238.

Friedlingstein, P., Cox, P., Betts, R., et al. 2006: Climate–Carbon Cycle Feedback Analysis: Results from the C4MIP Model Intercomparison. *Journal of Climate,* 19, 3337-3353.

Friedlingstein P, Dufresne JL, Cox PM, and Rayner P, 2003. How positive is the feedback between climate change and the carbon cycle? *Tellus,* 55B, 692–700.

Galloway, J. N., F. J. Dentener, D. G. Capone, E. W. Boyer, R. W. Howarth, S. P. Seitzinger, G. P. Asner, C. Cleveland, P. Green, E. Holland, D. M. Karl, A. F. Michaels, J. H. Porter, A. Townsend, and C. Vörösmarty. 2004. Nitrogen Cycles:ast, Present and Future. *Biogeochemistry* 70: 153-226.

Gordon, W.S., Famiglietti, J.S., 2004. Response of the water balance to climate change in the United States over the 20th and 21st centuries: results from the VEMAP Phase 2 model intercomparisons. *Global Biogeochemical Cycles* 18(GB1030) Doi: 10.1029/2003GB002098.

Greco, S., Baldocchi, D.D. 1996. Seasonal variations of $CO_2$ and water vapor exchange rates over a temperate deciduous forest. *Global Change Biology*. 2, 183-198.

Haefner, J. W. 2005. *Modeling biological systems: principles and applications* I, Springer.

Heimann, M. & Reichstein M. 2008. Terrestrial ecosystem carbon dynamics and climate feedbacks. *Nature,* 451, 289-292.

Houghton, R. A., Davidson, E. A., WoodwellG. M. 1998. Missing sinks, feedbacks, and understanding the role of terrestrial ecosystems in the global carbon balance. *Global Biogeochem. Cycles,* 12, 25–34.

Houghton, R.A., J.L. Hackler, and K.T. Lawrence. 1999. The U.S. Carbon budget: contributions from land-Use change. *Science* 285: 574-578.

Howell, T. A. 2001. Enhancing water use efficiency in irrigated agriculture *Agronomy Journal* 93, 281-289.

Hurtt, G.C., Pacala, S.W., Moorcroft, P.R., Caspersen, J.P., Shevllakova, E., Houghton, R.A., Moore, B., 2001. Projecting the future of the U.S. carbon sink. *Proceedings of the National Academy of Sciences* 99(3) 1389-1494.

Hyvonen, R., Agren, G. I., Linder, S., et al. 2007. The likely impact of elevated $CO_2$, nitrogen deposition, increased temperature and management on carbon sequestration in temperate and boreal forest ecosystems a literature review. *New Phytologist*, 173, 463-480

Janssens, I. A., Dieleman, W., Luyssaert, S., et al. 2010. Reduction of forest soil respiration in response to nitrogen deposition. *Nature Geoscience*, 3, 315-322.

Jackson, R.B., Cook, C.W., Pippen, J.S., Palmer, S.M., 2009. Increased belowground biomass and soil $CO_2$ fluxes after a decade of carbon dioxide enrichment in a warm-temperate forest. Ecology 90(12) 3352-3366.

Jackson, R. B., Jobbágy, E. G., Avissar, R., et al. 2005. Trading water for carbon with biological carbon sequestration, *Science*, 310, 1944.

Jones, C. D., Cox, P, M., Huntingford, C. 2006. Climate-carbon cycle feedbacks under stabilization: uncertainty and observational constraints. *Tellus*, 58B, 603-613.

Jung, M., Reichstein, M., Ciais, P., Seneviratne, S.I., Sheffield, J., Goulden, M.L., Bonan, G.B., Cescatti, A., Chen, J., deJeu, R., Dolman, A.J., Eugster, W., Gerten, D., Gianelle, D., Gobron, N., Heinke, J., Kimball, J., Law, B.E., Montagnani, L., Mu, Q., Mueller, B., Oleson, K., Papale, D., Richardson, A.D., Roupsard, O., Running, S., Tomelleri, E., Viovy, N., Weber, U., Williams, C., Wood, E., Zaehle, S., Zhang, K., 2010. Recent decline in the global land evapotranspiration trend due to limited moisture supply. *Nature* 467 951-954.

Karnosky, D.F., Pregitzer, K.S., Zak, D.R., Kubiske, M.E., Hendrey, G.R., Weinstein, D., Nosal, M. and Percy, K.E. 2005 Scaling ozone responses of forest trees to the ecosystem level in a changing climate. *Plant, Cell and Environment* 28, 965-981.

Katul, G.G., Ellsworth, D.S., Lai, C.T. 2000. Modelling assimilation and intercellular $CO_2$ from measured conductance: a synthesis of approaches. *Plant Cell Environment*, 23, 1313-1328.

Katz, R. W. 2002. Techniques for estimating uncertainty in climate change scenarios and impact studies. *Climate Research*, 20: 167-185.

Keller, M., Alencar, A., Asner, G.P., et al. 2004. Ecological research in the large-scale biosphereatmosphere experiment in Amazonia: Early results. Ecological Applications, 14, S3-S16.

Kooten, G. C., Grainger, A., Ley, E. 1997. Conceptual issues related to carbon sequestration: uncertainty and time. *Critical Reviews in Environmental Science and Technology*, 27(Special): S65-S82.

Korner C. 2000. Biosphere responses to $CO_2$ enrichment. *Ecological Application*, 10(6), 1590-1610.

LeBauer, D.S., Treseder, K.K., 2008. Nitrogen limitation of net primary productivity in terrestrial ecosystems is globally distributed. *Ecology* 89(2) 371-379.

Lichter, J, Lavine, M, Mace K.A, et al. 2000. Throughfall chemistry in a loblolly pine plantation under elevated atmospheric $CO_2$ concentrations. *Biogeochemistry*, 50, 73-93.

Liu, M., Tian, H., Chen, G., Ren, W., Zhang, C., Liu, J., 2008. Effects of land-use and land-cover change on evapotranspiration and water yield in China during 1900-2000. *Journal of the American Water Resources Association* 44(5) 1193-1207.

Lockwood, JG. 1999. Is potential evapotranspiration and its relationship with actual evapotranspiration sensitive to elevated atmospheric $CO_2$ levels? *Climate Change*, 41, 193-212.

Lu, C. 2009. *Atmospheric nitrogen deposition and terrestrial ecosystem carbon cycling* , PhD. Dissertation, Chinese Academy of Science, Beijing.

Mäkipää R., Karjalainen T., Pussinen A., Kellomäki S. 1999. Effects of climate change and nitrogen deposition on the carbon sequestration of a forest ecosystem in the boreal zone. *Can. J. Forest Res.* 29, p. 1490–1501.

Malmsheimer, R.W., Heffernan, P., Brink, S., Crandall, D., Deneke, F., Galik, C., Gee, E., Helms, J.A., Mcclure, N., Mortimer, M., Ruddell, S., Smith, M., Stewart, J., 2008. Forest management solution for mitigating climate change in the United States. *Journal of Forestry* 106(3) 115-118.

Margolis, H.A., Flanagan, L.B., Amiro, B.D. 2006. The fluxnet-Canada research network: Influence of climate and disturbance on carbon cycling in forests and peatlands. *Agricultural and Forest Meteorology*. 140, 1-5.

Massman W.J., and Grantz D. A. 1995. Estimating canopy conductance to ozone uptake from observations of evapotranspiration at the canopy scale and at the leaf scale. *Global Change Biology*, 1(3), 183-198.

Maurer E. P., L. Brekke, T. Pruitt, and P. B. Duffy 2007 'Fine-resolution climate projections enhance regional climate change impact studies', *Eos Trans*. AGU, 88(47), 504.

Maurer, S., Egli, P., Spinnler, D., et al. 1999. Carbon and water fluxes in Beech–Spruce model ecosystems in response to long-term exposure to atmospheric $CO_2$ enrichment and increased nitrogen deposition. *Functional Ecology*, 13, 748-755.

McGuire, A.D., Sitch,S., Clein, J.S., et al. 2001. Carbon balance of the terrestrial biosphere in the twentieth century: Analyses of $CO_2$, climate and land-use effects with four process-based ecosystem models. *Global Biogeochemical Cycles*, 15, 183-206.

Medvigy, D., Wofsy, S. C., Munger, J. W., et al. 2010. Responses of terrestrial ecosystems and carbon budgets to current and future environmental variability. *PNAS*, 107, 8275-8280.

Melillo, J.M., McGuire, A.D., Kicklighter, D.W., Moore B, I.I.I., Vorosmarty, C.J., Schloss, A.L., 1993. Global climate change and terrestrial net primary production. *Nature* 363 234-240.

Miller, D.A., White, R.A. 1998 A Conterminous United States Multi-Layer Soil Characteristics Data Set for Regional Climate and Hydrology Modeling. *Earth Interactions*, 2: [Online] URL: http://EarthInteractions.org.

Morales, P., Sykes M. T., I. COLIN PRENTICEw. 2005 Comparing and evaluating process-based ecosystem model predictions of carbon and water fluxes in major European forest biomes. *Global Change Biology* 11, 2211–2233, doi: 10.1111/j.1365-2486.2005.01036.x

Nadelhoffer, K., Emmett, B.A., Gundersen, P., Kjonaas, O.J., Koopmans, C.J., Schleppi, P., Tietema, A., Wright, R.F., 1999. Nitrogen deposition makes a minor contribution to carbon sequestration in temperate forests. *Nature* 398 145-148.

Neftel, A, Oeschger H, Schwander J, Stauffer B, Zumbrunn R. 1982. Ice core sample measurements give atmospheric $CO_2$ content during the past 40,000 yr. *Nature*, 295, 220–223.

Nemani R., Running, S. W., Band, L. E., et al., 1993: *Regional hydroecological simulation system: An illustration of the integration of ecosystem models in a GIS. Environmental Modeling with GIS*, edited by M. F. Goodchild, B. O. Parks, and L. T. Steyaert, Oxford University Press, New York, 296-304.

Norby, R.J., Luo, Y., 2004. Evaluating ecosystem responses to rising atmospheric $CO_2$ and global warming in a multi-factor world. *New Phytologist* 162 281-293.

Ollinger, S. V., Aber, J. D., Reich, P. B., et al. 2002. Interactive effects of nitrogen deposition, tropospheric ozone, elevated $CO_2$ and land use history on the carbon dynamics of northern hardwood forests. *Global Change Biology*, 8, 545-562.

Pataki, D.E., Oren, R., Tissue, D. 1998. Elevated carbon dioxide does not affect canopy stomatal conductance of Pinus taeda L. *Oecologia*, 117, 47-52.

Prentice I.C., Farquhar G.D., Fasham M.J.R., Goulden M.L., Heimann M, Jaramillo V.J., Kheshgi H.S., Le Quere C., Scholes R.J., Wallace D.W.R. 2001. The carbon cycle and atmospheric carbon dioxide. In: Houghton J.T., Ding Y., Griggs D.J., Noguer M, van der Linden

P.J., Dai X, Mashell K, Johnson C.A., eds. Climate change 2001: the scientific basis, Cambridge, UK: Cambridge University Press, 183-237.

Ramankutty, N., Foley J.A. 1998 Characterizing patterns of global land use: An analysis of global croplands data. *Global Biogeochem Cycles*. 12:667–685.

Randerson, J. T., Thompson, M. V., Conway, T. J., et al. 1997. The contribution of terrestrial sources and sinks to trends in the seasonal cycle of atmospheric carbon dioxide. *Global Biogeochem. Cycles*, 11, 535–560.

Rastetter, E.B., Agren, G.I., Shaver, G.R., 1997. Responses of N-limited ecosystems to increased $CO_2$: a balanced-nutrition, coupled-element-cycles model. Ecological Applications 7(2) 444-460.

Ren, W., H. Tian, M. Liu, C. Zhang, G. Chen, S. Pan, B. Felzer, and X.F. Xu .2007. Tropospheric ozone pollution and its influence on net primary productivity and carbon storage in terrestrial ecosystems of China. *Journal of Geophysical Research*, 112, D22S09, DOI: 10.1029/2007JD008521.

Running, S. W. 1994. Testing Forest-BGC ecosystem process simulations across a climatic gradient in Oregon. *Ecol. Appl*., 4, 238–247.

Schäfer, K.V.R., Oren, R., Lai, C.T., et al. 2002. Hydrologic balance in an intact temperate forest ecosystem under ambient and elevated atmospheric $CO_2$ concentration. *Global Change Biology*, 8, 895-911.

Schimel, D. S., Melillo, J., Tian, H., et al. 2000. Contribution of increasing $CO_2$ and climate to carbon storage by ecosystems in the United States. *Science*, 287, 2004–2006.

Schlesinger, W.H., 1997. *Biogeochemistry: An analysis of global change*. Academic Press, New York.

Shackley, S., Young, P., Parkinson, S., et al. 1998. Uncertainty, complexity and concepts of good science in climate change modeling: are GCMs the best tools? *Climatic Change*, 38, 159-205.

Sitch, S., Cox, P. M., Collins, W. L., et al. 2007. Indirect radiative forcing of climate change through ozone effects on the land-carbon sink, *Nature*, 448, doi:10.1038/nature06059.

Solomon, S., Qin, D., Manning, M., Alley, R.B., Berntsen, T., Bindoff, N.L., Chen, Z., Chidthaisong, A., Gregory, J.M., Hegerl, G.C., Heimann, M., Hewitson, B., Hoskins, B.J., Joos, F., Jouzel, J., Kattsov, V., Lohmann, U., Matsuno, T., Molina, M., Nicholls, N., Overpeck, J., Raga, G., Ramaswamy, V., Ren, J., Rusticucci, M., Somerville, R., Stocker, T.F., Whetton, P., Wood, R.A., Wratt, D., 2007. Techical summary, In: Solomon, S., Qin, D., Manning, M., Chen, Z., Marquis, M., Averyt, K.B., Tignor, M., Miller, H.L. (Eds.), *Climate Change 2007: The Physical Science Basis. Contribution of Working Group I to the Fourth Assessment Reprot of the Intergovernmental Panel on Climate Change:* Cambridge, United Kingdom and New York, NY, USA.

Thomas, R. Q., Canham, C. D., Weathers, K. C., et al. 2010. Increased tree carbon storage in response to nitrogen deposition in the US. *Nature Geoscience*, 3, 13-17.

Tian, H., Melillo, J.M., Kicklighter, D.W., McGuire, A.D., Helfrich III, J.V.K., Moore III, B., Vörösmarty, C.J. 1998. Effect of interannual climate variability on carbon storage in Amazonian ecosystems. *Nature* 396, 664-667.

Tian, H.Q. 2002. Modeling dynamics of the terrestrial biosphere in changing global environments: models, data, and validation. *J. of Geographical Science* 57, 378-388.

Tian, H., J.M. Melillo, D.W. Kicklighter, S. Pan, J. Liu, A.D. McGuire, and B. Moore III. 2003. Regional carbon dynamics in monsoon Asia and its implications to the global carbon cycle. *Global and Planetary Change* 37: 201-217.

Tian, H., X. Xu, C. Zhang, W. Ren, G. Chen, M. Liu, D. Lu, and S. Pan, 2008. Forecasting and Assessing the Large-scale and Long-term Impacts of Global Environmental Change on Terrestrial Ecosystems in the United States and China. In: Miao, S., S. Carstenn, and M. Nungesser, Eds. *Real World Ecology: large-scale and long-term case studies and methods*. Springer, New York.

Tian, H., G. Chen, M. Liu, C. Zhang, G. Sun, C. Lu, X. Xu, W. Ren, S. Pan, A. Chappelka. 2010a. Model estimates of net primary productivity, evapotranspiration, and water use efficiency in the terrestrial ecosystems of the southern United States during 1895-2007. *Forest Ecology and Management* 259: 1311-1327.

Tian, H., Xu, X., Liu, M., Ren, W., Zhang, C., Chen, G., Lu, C., 2010b. Spatial and temporal patterns of $CH_4$ and $N_2O$ fluxes in terrestrial ecosystems of North America during 1979-2008: application of a global biogeochemistry model. *Biogeosciences* 7 2673-2694.

Tian, H., J.M. Melillo, C. Lu, D.W. Kicklighter, M. Liu, J. Liu, W. Ren, X. Xu, G. Chen, C. Zhang, S. Pan, S. Running. 2010c. Contributions of multiple global change factors to terrestrial carbon balance in China. *Global Biogeochemical Cycles*. In revision.

Turner D.P., G.J. Koerper, M.E. Harmon, and J.J. Lee. 1995. A carbon budget for forests for the conterminous United States. *Ecological Applications*, 5, 421-436.

Valentini, R., DeAngelis, P., Matteucci, G., et al. 1996. Seasonal net carbon dioxide exchange of a beech forest with the atmosphere. *Global Change Biology*, 2, 199-207.

Valentini, R., Matteucci, G., Dolman, A.J., et al. 2000. Respiration as the main determinant of carbon balance in European forests. *Nature*, 404, 861 - 865.

Vitousek, P.M., Mooney, H.A., Lubchenco, J., Melillo, J.M., 1997. Human domination of Earth's ecosystems. *Science* 277(5325) 494.

Vitousek, P. M., and Howarth, R. W. 1991. Nitrogen limitation on land and in the sea-How can it occur? *Biogeochemistry*, 13:87–115.

Waisanen, P.J., Bliss, N.B. 2002 Changes in population and agricultural land in conterminous United States counties, 1790 to 1997. *Global Biogeochemical Cycles* 16, 1137

Wear, D.N., and J.G. Greis. 2002. Southern Forest Resource Assessment. General Technical Report SRS-53. Asheville, NC: USDA Forest Service, Southern Research Station. 635 p.

Wofsy, S.C., Goulden, M.L., Munger, J.W., et al. 1993. Net exchange of $CO_2$ in a midlatitude forest. *Science*, 260, 1314-1317.

Wullschleger, S.D, Norby, RJ. 2001. Sap velocity and canopy transpiration in a sweetgum stand exposed to free-air $CO_2$ enrichment (FACE). *New Phytologist*, 150, 489-98.

Xu, L.K., Hsiao, T.C. 2004. Predicted versus measured photosynthetic water-use efficiency of crop stands under dynamically changing field environments. *Journal of Experimental Botany*, 55: 2395-2411.

Xu, X., Tian, H., Zhang, C., Liu, M., Ren, W., Chen, G., Lu, C., Bruhwiler, L., 2010. Attribution of spatial and temporal variations in terrestrial ecosystem methane flux over North America. Biogeosciences 7 3637-3655.

Yamamoto, S., Murayama, S., Saigusa, N., et al. 1999. Seasonal and inter-annual variation of $CO_2$ flux between a temperate forest and the atmosphere in Japan. *Tellus*, 51B, 402-413.

Yu, G., Wang, Q., Zhuang, J. 2004. Modeling the water use efficiency of soybean and maize plants under environmental stresses: application of a synthetic model of photosynthesis–transpiration based on stomatal behavior. *Journal of Plant Physiology*, 161: 308–318.

Yu, G., Song, Xia., Wang, Qiufeng., et al. 2008.Water-use efficiency of forest ecosystems in eastern China and its relations to climatic variables. *New Phytologist*, 177: 927-937.

Yu, G., Wen, X., Sun, X., et al. 2006. Overview of chinaflux and evaluation of its eddy covariance measurement. *Agricultural and Forest Meteorology*, 137, 125-137.

Zhang C. 2008. Terrestrial carbon dynamics of southern United States in response to changes in climate, atmosphere, and land use/land cover from 1895 to 2005. Dissertation, School of Forestry and Wildlife Sciences, Auburn University.